

June 27, 2011

Tinkertoys for the D_N series

Oscar Chacaltana and Jacques Distler

*Theory Group and
Texas Cosmology Center
Department of Physics,
University of Texas at Austin,
Austin, TX 78712, USA*

Email: oscarch@physics.utexas.edu
Email: distler@golem.ph.utexas.edu

Abstract

We describe a procedure for classifying 4D $\mathcal{N} = 2$ superconformal theories of the type introduced by Davide Gaiotto. Any punctured curve, C , on which the 6D $(2, 0)$ SCFT is compactified, may be decomposed into 3-punctured spheres, connected by cylinders. The 4D theories, which arise, can be characterized by listing the “matter” theories corresponding to 3-punctured spheres, the simple gauge group factors, corresponding to cylinders, and the rules for connecting these ingredients together. Different pants decompositions of C correspond to different S-duality frames for the same underlying family of 4D $\mathcal{N} = 2$ SCFTs. In a previous work [1], we developed such a classification for the A_{N-1} series of 6D $(2, 0)$ theories. In the present paper, we extend this to the D_N series. We outline the procedure for general D_N , and construct, in detail, the classification through D_4 . We discuss the implications for S-duality in $Spin(8)$ and $Spin(7)$ gauge theory, and recover many of the dualities conjectured by Argyres and Wittig [2].

Contents

1	Introduction	1
2	The D_N Series	3
2.1	Punctures and the Spaltenstein Map	5
2.2	Irregular Punctures	10
2.3	Central charges	11
2.4	Regular Punctures (up through D_6)	15
2.4.1	D_3	15
2.4.2	D_4	16
2.4.3	D_5	17
2.4.4	D_6	18
3	The D_4 theory	21
3.1	Irregular punctures and cylinders	21
3.2	Fixtures	23
3.2.1	Free-field fixtures	24
3.2.2	Interacting fixtures	26
3.2.3	Mixed fixtures	30
3.3	The $Sp(4)_8 \times Sp(2)_7$ and $Sp(5)_7$ SCFTs	31
3.3.1	$Sp(4)_8 \times Sp(2)_7$ SCFT	31
3.3.2	$Sp(5)_7$ SCFT	33
4	$Spin(8)$ Gauge Theory	36
4.1	$2(8_s) + 2(8_c) + 2(8_v)$	37
4.2	$3(8_s) + 2(8_c) + 8_v$	38
4.3	$3(8_s) + 3(8_c)$	40
4.4	$4(8_s) + 2(8_c)$	41
4.5	$4(8_s) + 8_c + 8_v$	42
4.6	Seiberg-Witten curves	42
5	$Spin(7)$ Gauge Theory	43
5.1	$2(8) + 3(7)$	43
5.2	$3(8) + 2(7)$	43
5.3	$4(8) + 1(7)$	44
5.4	$5(8)$	44
6	Other Interesting Examples	45
6.1	Fun with interacting SCFTs	45
6.2	D_5 example: $Spin(10)$ gauge theory	47
A	Appendix: Nilpotent orbits in $\mathfrak{so}(2N)$	50

1. Introduction

Gaiotto duality [3,4,5,6,7,1,8,9,10] identifies a large class of 4D $\mathcal{N} = 2$ SCFTs with compactifications of the 6D $\mathcal{N} = (2, 0)$ SCFT on a punctured Riemann surface, C . The moduli space, $\mathcal{M}_{g,n}$, parametrizes the family of exactly-marginal deformations of the SCFT. For every pants-decomposition of C , there is an $\mathcal{N} = (2, 0)$ gauge-theoretic interpretation, in which each cylinder represents the $\mathcal{N} = 2$ vector multiplets for some (simple) gauge group, and the 3-punctured spheres represent some sort of “matter”, charged under the gauge groups of the attached cylinders. In particular, this construction identifies the boundaries of the moduli space, $\mathcal{M}_{g,n}$, with limits in which some, or all, of the gauge couplings become weak. Different degenerations correspond to different, S-dual, realizations of the same family of SCFTs.

Classifying the theories that arise, in this way, comes down to specifying (for a given 6D (2,0) theory) what all of the 3-punctured spheres are, what gauge groups are associated with the cylinders that connect them, and what are the rules for gluing these ingredients together. Arbitrarily complicated 4D $\mathcal{N} = 2$ SCFTs can be constructed, in “tinkertoy” fashion, by connecting together these basic ingredients.

For a given (2,0) theory, this is a finite task. In our previous paper [1], we carried out this program for theories that are obtained from a compactification of the (2,0) theories of type A_{N-1} . In so-doing, we identified a multitude of new interacting, non-Lagrangian SCFTs (generalizing [11]), corresponding to compactifications of the A_{N-1} theory on certain 3-punctured spheres. Their appearance, in the context of Gaiotto duality, is a vast generalization of the classic examples of non-Lagrangian SCFTs appearing in the S-dual description of more-familiar $\mathcal{N} = 2$ gauge theories, discovered by Argyres and Seiberg [12].

While Gaiotto’s original arguments relied on the realization of the 6D theory as the low-energy theory of N M5-branes, which necessarily implied working with a 6D theory of A_{N-1} type, the idea can be straightforwardly generalized to the case of N M5 branes in the presence of an orientifold, whose low-energy limit is the 6D theory of type D_N . (There is, by contrast, no realization of the 6D theories of type E as a low-energy theory of M5 branes.) The class of 4D SCFTs arising from the compactification of the D_N 6D theories on Riemann surfaces has been considerably less studied [8,9,10] than its A_{N-1} analogue.

As for the A_{N-1} theories, the Seiberg-Witten curve of 4D theories arising from the D_N theories can be written in Gaiotto’s form, as a polynomial equation in the Seiberg-Witten differential (a 1-form on T^*C), whose coefficients are (the pullbacks of) differentials on C . The differentials descend from protected operators of the 6D theory, and so their degrees are equal to the exponents of $Spin(2N)$.

Just as Gaiotto used the well-known $SU(n)$ linear quivers to test his arguments for the A_{N-1} theory, Tachikawa [8,9] studied the SO-Sp linear quivers [13,14] to find the pole structure and flavour symmetry group for punctures in the D_N theory, and discovered a few examples of S-duality. Unfortunately, the SO-Sp linear quivers, that arise from the orientifold construction, live in a theory slightly larger than the one we are interested in. The A_{N-1} , D_N and E_6 theories have a \mathbb{Z}_2 outer-automorphism (which gets enhanced to S_3 in the case of D_4), and we can consider compactifications of the (2,0) theory, where going around a homologically-nontrivial cycle on C (circumnavigating a handle, or circling

a puncture) is accompanied by an outer-automorphism twist.

A proper discussion of the incorporation of outer-automorphism twists should treat the A_{N-1} , D_N and E_6 (2,0) theories in tandem, as all of these Dynkin diagrams have a \mathbb{Z}_2 outer automorphism. We will leave that discussion to a forthcoming paper. Instead, in this paper, we will study the compactifications of the D_N theory, *without* outer-automorphism twists, and develop a classification precisely analogous to the one we developed for the A_{N-1} theory (also without outer automorphism twists). Nonetheless, at a crucial point, we will have recourse to Tachikawa’s linear quiver tail analysis which, strictly speaking, embeds the D_N theories without outer automorphism twists in the larger class of D_N theories which *do* include outer automorphism twists.

The analysis in the D_N case introduces several new complications, not seen in the A_{N-1} case. In the A_{N-1} theory, each puncture corresponded to a choice of partition of N (equivalently, to an N -box Young diagram, or a nilpotent orbit in the complexified Lie algebra, $\mathfrak{sl}(N)$). The chosen partition determined the “flavour symmetry” group (essentially, the isometry group of the Higgs branch) associated to a given puncture. At the same time, it (or, more accurately, its transpose) determined the singular behaviour of the Hitchin system at the puncture which, in turn, gave the geometry of the Coulomb branch.

In the present case, that relationship is more complicated. As in the A_{N-1} case, the flavour symmetry group (geometry of the Higgs branch) is determined by a “D-partition” of $2N$. Such partitions also label nilpotent orbits in $\mathfrak{so}(2N)$. However, only for a subset of these, the “special” D-partitions [15], is the behaviour of the Hitchin system at the puncture given by (the Spaltenstein dual) nilpotent orbit.

The Coulomb branch of the theory comprises the degrees of freedom associated to a set of meromorphic k -differentials on the Riemann surface which are allowed to have poles of certain orders (determined by the choice of partition) at the punctures. A new feature, of the D_N case, is that the coefficients of the leading poles of these differentials obey certain polynomial constraints. The “true” Coulomb branch is obtained, after imposing the constraints.

These constraints were derived by Tachikawa [8], by considerations involving linear quiver tails. We will present a slightly different, more intrinsic, viewpoint on the origin of these constraints. For the special partitions, we will see that the constraints pop out naturally from requiring that the Higgs field have a simple pole with residue lying in the Spaltenstein-dual nilpotent orbit. For the non-special partitions, our results are less satisfactory. We can determine (using the linear quiver tail analysis) the pole structure of the k -differentials at the puncture, and the associated constraints. But we do not, currently, know how to express this as a boundary condition of the Hitchin system.

A further peculiar feature of the non-special punctures is that the global symmetry group of the puncture contains $Sp(l)_k$ factors, with k odd. This level for the current algebra is that which would be induced by an odd number of half-hypermultiplets in the fundamental $2l$ -dimensional representation. In other words, this symmetry is subject to Witten’s global anomaly [16] and (in the absence of additional matter) could not be consistently gauged.

Even after having dealt with these new complexities, simply enumerating the *results* in the D_N case is considerably more tedious than it was in the A_{N-1} case. The number of fixtures (3-punctured spheres), and the number of cylinders that connect them, proliferate much more rapidly with N .

We will restrict ourselves to presenting a complete catalogue only for D_4 . As a measure of the complexity, there are 99 3-punctured spheres for D_4 ; we will list all of those. There are 785 4-punctured spheres — theories with a single gauge group factor — it would be prohibitive to list all of those.

Nevertheless D_4 is an interesting case to study. As already mentioned, the outer automorphism group is enhanced to S_3 . This group is a symmetry of the D_4 (2,0) theory, and so acts on the set of punctures/fixtures/cylinder, which are naturally organized into multiplets, permuted by the outer automorphisms. As already mentioned, we will *not* consider the inclusion of outer-automorphism *twists*.

For the D_5 and D_6 theories, we will present tables of the regular punctures and their properties, but will refrain from presenting a complete catalogue of fixtures and cylinders.

As in the A_{N-1} series, we discover several new interacting SCFTs — non-Lagrangian fixed points of the renormalization group — and we realize a number of S-dualities predicted by Argyres and Wittig [2]. We also provide formulæ for the conformal-anomaly central charges a, c , and explain how to compute the flavour current-algebra charges k , for interacting SCFTs.

2. The D_N Series

Much of the construction is well-reviewed in previous works [3,4,8,9,7,6,17,10], so we will be somewhat brief, concentrating on the novelties which arise in the D_N case. We consider a 6D (2,0) theory compactified on a Riemann surface C of genus g with n punctures (complex codimension-1 defect operators) located at points $y_i \in C$, $i = 1, \dots, n$.

In the A_{N-1} case, the Seiberg-Witten curve, $\Sigma \subset T^*C$ of the 4d low-energy theory is given by

$$0 = \lambda^N + (-1)^N \sum_{k=2}^N \lambda^{N-k} \phi_k(y), \quad (1)$$

where λ is the Seiberg-Witten differential, and the $\phi_k(y)$ are k -differentials on C (pulled back to T^*C). The ϕ_k are allowed to have poles of various orders at the y_i .

The theory possesses a set of relevant operators, whose vacuum expectation values parametrize the Coulomb branch of the theory. At a generic point on the Coulomb branch, the theory is infrared-free; at the origin, it is superconformal. The tangent space at the origin of the Coulomb branch is a graded vector space,

$$V = \bigoplus_{k=2}^N V_k. \quad (2)$$

where $V_k = H^0\left(C, K^k\left(\sum_{i=1}^n p_k^{(i)} y_i\right)\right)$ is the vector space of meromorphic k -differentials, ϕ_k , with poles of order at most p_k^i at the punctures y_i .

As we vary the gauge couplings, the graded vector spaces, V , fit together to form the fibers of a graded vector bundle over the moduli space, $\mathcal{M}_{g,n}$, of marginal-deformations. Our main guiding principle is that this vector bundle should extend to the boundary of $\mathcal{M}_{g,n}$. What naturally extends, over $\overline{\mathcal{M}}_{g,n}$, are the virtual bundles whose fibers are

$$H^0\left(C, K^k\left(\sum_{i=1}^n p_k^{(i)} y_i\right)\right) \ominus H^1\left(C, K^k\left(\sum_{i=1}^n p_k^{(i)} y_i\right)\right) \quad .$$

We will arrange for the H^1 s to vanish, so that the virtual bundle is an honest bundle, which extends to the boundary. At the boundary, the Coulomb branch has components associated to the irreducible components of C and components associated to the gauge groups on the degenerating cylinders.

For the D_N series of $(2, 0)$ theories, the story is superficially similar. The Seiberg-Witten curve takes the form

$$0 = \lambda^{2N} + \sum_{k=1}^{N-1} \lambda^{2(N-k)} \phi_{2k}(y) + \tilde{\phi}^2(y) \quad (3)$$

Again, the ϕ_{2k} and $\tilde{\phi}$ are meromorphic differentials on C , with poles of up to the prescribed orders at the punctures. ($\tilde{\phi}$ is the Pfaffian, i.e., an N -differential.)

However, there are some crucial differences between the A_{N-1} and D_N theories. While in the A_{N-1} case, the coefficients in the Seiberg-Witten equation (1) were just linear functions of the Coulomb branch (2), in the D_N case, the coefficients in Seiberg-Witten equation (3) are, in general, polynomial expressions when expressed in terms of the natural linear coordinates at the origin of the Coulomb branch. We see that, already, in the fact that the Seiberg-Witten equation depends quadratically on $\tilde{\phi}$. But there are further polynomial constraints on the coefficients in the ϕ_{2k} , which need to be solved before one sees the natural linear structure.

While the constraints are polynomial, they are always *linear* in (at least) *one* of the variables. Moreover, they are of homogeneous degree in the aforementioned grading. So the space of solutions of the constraints is always smooth at the origin of the Coulomb branch, and hence the tangent space at the origin has the desired structure of a graded vector space.

The other complication in the D_N theories is that, whereas the differentials in the D_N theory have degrees $2, 4, 6, \dots, 2(N-1)$; N , the Coulomb branch has components in other degrees. For instance, in D_4 , there is a component of degree 3, in addition to the “expected” components of degrees 2, 4, 6. In general, the Coulomb branch takes the form

$$E \subset V$$

where

$$V = \bigoplus_{k=1}^{N-1} H^0\left(C, K^{2k}\left(\sum_{i=1}^n p_i^{(k)} y_i\right)\right) \oplus \bigoplus_{k=3}^{N-1} W_k \oplus H^0\left(C, K^N\left(\sum_{i=1}^n \tilde{p}_i y_i\right)\right)$$

Here the W_k are vector spaces of degree k and E is the subvariety satisfying the collection of polynomial constraints (linear in at least one variable, and of homogeneous degree).

If we denote the coefficient of l^{th} -order pole of ϕ_k , at one of the punctures, by $c_l^{(k)}$, the constraints can roughly be divided into

- polynomials (of homogeneous degree in both k and l) in the $c_l^{(k)}$
- polynomials (again, of appropriately homogeneous degree) involving both the $c_l^{(k)}$ and a basis $a^{(k)}$ for the vector spaces, W_k

In the case of D_4 , there is just W_3 , and $\dim(W_3) = n_o$, the number of punctures, on C , corresponding to a particular special D-partition. At each such puncture, there is a constraint $c_4^{(6)} = (a^{(3)})^2$, which says that the coefficient of the leading singularity of ϕ_6 is a perfect square. As we will elaborate later, there is a unique non-special nilpotent orbit of D_4 . The puncture in question is the image, under the Spaltenstein map, of that non-special nilpotent orbit.

2.1. Punctures and the Spaltenstein Map

In the A_{N-1} series, punctures are labeled by partitions of N . To each such partition, $[h_1, h_2, \dots, h_p]$, with

$$h_1 \geq h_2 \geq \dots \geq h_p$$

$$\sum_{i=1}^p h_i = N,$$

we associated a Young diagram, whose i^{th} column has height h_i . The corresponding flavour symmetry group is

$$G = S \left(\prod_h U(n^{(h)}) \right) \quad (4)$$

where $n^{(h)}$ is the number of columns of height h . Of course, a Young diagram with N boxes determines a second partition of N , given by the row-lengths, $[r_1, r_2, \dots, r_q]$. The two partitions are said to be transposes of each other, as the map between them consists of taking the transpose of the Young diagram.

This second partition determines a nilpotent orbit [15], $\mathcal{O}_{[r_1, r_2, \dots, r_q]} \subset \mathfrak{sl}(N)$, which determines the pole structure of the $\phi_k(y)$ at the puncture. Specifically, the Higgs field of the Hitchin system (obtained upon further compactifying the theory on a circle) has a simple pole, with residue $X \in \mathcal{O}_{[r_1, r_2, \dots, r_q]}$ at the puncture [18,4,7]. There's a fairly simple algorithm for choosing such a representative, X :

- Let X be a block-diagonal matrix, where the i^{th} block is $r_i \times r_i$.
- Within each block, let X be strictly upper-triangular.

The characteristic equation

$$\det(\varphi(y) - q\mathbb{1}) = (-q)^N + \sum_{k=2}^N q^{N-k} \phi_k(y) \quad (5)$$

(for generic finite part of φ) determines the allowed pole orders of the ϕ_k . The result is easily-expressed in terms of the corresponding Young diagram:

- Starting with 0 in the first box, number the boxes in the first row with successive positive integers.
- When you get to the end of a row, repeat that integer as the number assigned to the first box of the succeeding row. Continue numbering the boxes of that row with successive integers.
- The integers inscribed in boxes $2, \dots, N$ are, respectively, the pole orders of ϕ_2, \dots, ϕ_N .

For the D_N series, punctures are labeled by partitions of $2N$. However, not all partitions are allowed.

- Even integers must occur with even multiplicity.
- When all the integers in the partition are even (such a partition is called “very even”), we get *two* punctures. Such partitions only occur for N even. These two punctures are exchanged by the \mathbb{Z}_2 outer automorphism of D_N which exchanges the two spinor representations. We will colour the corresponding Young diagrams red and blue, to distinguish them.

Such a partition is called a “D-partition of $2N$.” As we shall see, presently, nilpotent orbits in $\mathfrak{so}(2N)$ are labeled by D-partitions of $2N$. We will also have recourse to a C-partition of $2N$ (related, as it happens, to nilpotent orbits in $\mathfrak{sp}(N)$), which has the property that odd integers occur with even multiplicity.

From the Young diagram, corresponding to a D-partition, we reconstruct the flavour symmetry group, associated to the puncture.

$$G = \prod_{h \text{ odd}} Spin(n^{(h)}) \times \prod_{h \text{ even}} Sp\left(\frac{n^{(h)}}{2}\right) \quad (6)$$

From this, the necessity of the rule that $n^{(h)}$ be even, for even h , is obvious. The origin of the additional rule (which arises for N even) — that “very even” D-partitions occur twice — has a more subtle origin.

For N odd, the irreducible spinor representation of D_N is complex, and the right-handed spinor representation is the complex-conjugate of the left-handed one. So a “hypermultiplet in the spinor” contains fields transforming as spinors of both chiralities.

For N even, the irreducible spinor representation is real ($N = 4l$) or pseudoreal ($N = 4l + 2$), and the left- and right-handed spinor representations are inequivalent. So a “hypermultiplet in the left-handed spinor representation” is *different* from a “hypermultiplet in the right-handed spinor representation.” When we discuss fixtures, we will need to keep track of this distinction. Exchanging “red” and “blue” punctures will exchange the roles of left- and right-handed spinors.

Understanding the singularities of the ϕ_k at the puncture is somewhat more involved than in the A_{N-1} case.

As in the A_{N-1} case, we might expect to associate a nilpotent orbit in $\mathfrak{so}(2N)$ to the rows of the Young diagram. Unfortunately, when the *columns* of a $2N$ -box Young diagram

form a D-partition, the *rows* typically do not. In other words, the transpose does not map D-partitions to D-partitions. Nevertheless, there is a simple modification of the transpose map, called the “Spaltenstein map” which *does* map D-partitions to D-partitions.

This procedure may be described as (row) “D-collapse”:

- Given a Young diagram whose columns form a D-partition, take the longest even row, which occurs with odd multiplicity (if the multiplicity is greater than 1, take the *last* row of that length), and remove the last box. Place the box at the end of the next available row, such that the result is a Young diagram.
- Repeat the process with next longest even row, which occurs with odd multiplicity.
- This process eventually terminates, and the result is a “corrected” Young diagram, whose row-lengths form a D-partition.

Conversely, starting with a Young diagram whose rows form a D-partition (thus specifying a nilpotent orbit), we can define a process of *column D-collapse*, which yields a Young diagram whose columns form a D-partition (hence, a flavour symmetry group).

In the A_{N-1} case, the Spaltenstein map was given by transpose (alternatively by reading the partition from the rows/columns instead of columns/rows of the Young diagram). In the D_N case, the Spaltenstein map is defined as the composition of the transpose with the appropriate (row/column) D-collapse. Unfortunately, unlike the transpose, the Spaltenstein map is *not* an involution of the set of D-partitions; in general, it is neither 1-1 nor onto. The set of partitions in the image of the Spaltenstein map are called “special”, and the Spaltenstein map, restricted to the special partitions, *is* an involution.

More formally, let s be the Spaltenstein map, and let p be a D-partition. p is called “special” if $s^2(p) = p$. In the A_{N-1} case, all partitions were special ($(p^t)^t = p$). That’s not the case for D_N . Instead, we have the theorem

Theorem 1. ([15] Corollary 6.36 and Proposition 6.3.7)

1. For any D-partition, p , $s(p)$ is a special D-partition.
2. A D-partition, p , is special, if and only if p^t is a C-partition.


The boundary conditions for the punctures corresponding to special D-partitions are determined as in the A_{N-1} case. Let f be the D-partition which gives the flavour symmetry. Let $o = s(f)$ be the image of f under the Spaltenstein map. If f is special (which was *always* the case for A_{N-1}), then the Higgs field $\varphi(y)$ has a simple pole, with residue $X \in o$. Under the obvious embedding $\mathfrak{so}(2N) \hookrightarrow \mathfrak{sl}(2N)$, the characteristic equation

$$\det(\varphi(y) - q\mathbb{1}) = q^{2N} + \sum_{k=1}^{N-1} q^{2(N-k)} \phi_{2k}(y) + (\tilde{\phi}(y))^2 \quad (7)$$

yields the pole orders of the k -differentials. These can be read off from the Young diagram for o , just as if it were a Young diagram for A_{2N-1} (see the rule above). Because $\varphi(y)$ lies in the $\mathfrak{so}(2N)$ subalgebra, the ϕ_k vanish for odd k , and $\phi_{2N}(y) = (\tilde{\phi}(y))^2$. That, however,

does not quite exhaust the constraints on the polar parts of the k -differentials, which follow from restricting to $\mathfrak{so}(2N) \subset \mathfrak{sl}(2N)$. There are additional polynomial constraints among the coefficients of the leading-order poles of the various k -differentials.

These additional constraints were previously found by Tachikawa [8] by applying the restrictions, imposed by M-theory orientifolds [19], to SO-Sp linear quiver tails. As already mentioned, the SO-Sp quivers naturally live in the larger theory, with outer-automorphism twists. From our present perspective it is better to think of the constraints as coming directly from putting the polar part of $\varphi(y)$ in a special nilpotent orbit of $\mathfrak{so}(2N)$. (For our explicit conventions on nilpotent orbits in $\mathfrak{so}(2N)$, see §A.)

As a simple example, consider the minimal D_3 puncture, . To find its pole structure, we put the polar part of the Higgs field in the nilpotent orbit of the Spaltenstein dual,



We write $\varphi(y) = \frac{X}{y} + M$, where $X = X_{1,2}^-$ is the canonical nilpotent element in this orbit (see §A for our conventions), and M is a generic matrix in $\mathfrak{so}(2N)$, of the form (40). The differentials are thus of the form

$$\phi_2 = \frac{2a}{y} + \dots, \quad \phi_4 = \frac{a^2}{y^2} + \dots, \quad \tilde{\phi} = \frac{b}{y} + \dots \quad (8)$$

Thus, the pole structure is $\{1, 2; 1\}$, with a constraint $c_2^{(4)} = \frac{1}{4}c_1^{(2)}$. This pole structure and constraint was computed in [8] from the SO-Sp linear quiver tail for this puncture.

That takes care of the punctures corresponding to special D-partitions. What about the punctures corresponding to non-special D-partitions? Here the situation is a bit more awkward. The Spaltenstein map is not an involution, when applied to non-special partitions, and so the boundary conditions on $\varphi(y)$ are not currently known. (This is currently under investigation [20].) The effect on the pole structure of the k -differentials, however, is easy to find (say, from the linear quiver tail analysis), and amounts to the following. Given a non-special D-partition, f , $f_s = s^2(f)$ is a special D-partition. The pole structure of the $\phi_k(y)$ is precisely that one would find for the puncture f_s . However, f_s has a series of constraints of the form $c_{2l}^{(2k)} = (a^{(k)})^2$ on the leading pole coefficients. For the puncture, f , some (or all) of these constraints are relaxed.

To see which constraint(s) are relaxed, notice that f is related to f_s by a process of (row) C-collapse. That is, we remove the last box from a row of odd length (which occurred with odd multiplicity) and place it lower-down on the Young diagram. The box we removed was an odd-numbered box (call it $2k+1$). By removing it, an even-numbered box (box $2k$) becomes the last box in that row. The puncture, f_s , had a constraint of the form $c_{2l}^{(2k)} = (a^{(k)})^2$. For each $(2k)^{\text{th}}$ box, thus exposed, we relax the corresponding constraint of f_s .

For D_4 , there is just one non-special puncture and, correspondingly, just one constraint that gets relaxed. We will defer a complete discussion to [20].

Finally, let us elaborate on our conventions for “very even” punctures. When N is even, the Pfaffian, $\tilde{\phi}$ has the same degree as ϕ_N . The outer-automorphism of D_N , which exchanges the roles of the two spinor representations, takes

$$\begin{aligned}\tilde{\phi} &\mapsto -\tilde{\phi} \\ \phi_{2k} &\mapsto \phi_{2k}, \quad k = 1, \dots, N-1\end{aligned}\tag{9}$$



For most punctures, the constraints are such that there is a unique Coulomb branch parameter (the coefficient of the highest-order pole of one of the ϕ_{2k}) which appears linearly. We can take that to be the variable eliminated by the constraint, so for the purpose of counting the graded dimension of the Coulomb branch, it is as if we simply reduced the allowed pole-order for that differential by 1.

The red/blue punctures are an exception. At a (a certain subset of) red/blue punctures, both $\tilde{\phi}$ and ϕ_N are allowed to have poles of some order (say, l) but a linear combination of the coefficients, $c_l^{(N)} \pm 2\tilde{c}_l$, is the variable that appears linearly in the associated constraints. Our convention¹ will be that, at a red regular puncture, the constraint is of the form

$$c_l^{(N)} + 2\tilde{c}_l = \dots\tag{10}$$

At the corresponding blue regular puncture, the constraint is

$$c_l^{(N)} - 2\tilde{c}_l = \dots\tag{11}$$

As an example, let us look at the punctures with flavour Young diagrams  and . Their nilpotent orbits correspond to these same Young diagrams, and the canonical nilpotent elements (see §A) are $X^{(r)} = X_{1,2}^- + X_{3,4}^-$ and $X^{(b)} = X_{1,2}^- + X_{3,4}^+$, respectively. After writing $\varphi(y) = \frac{X^{(r/b)}}{y} + M$ for the Higgs field, with M a generic $\mathfrak{so}(2N)$ matrix, we find for the differentials,

$$\begin{aligned}\phi_2 &= \frac{2a}{y} + \dots \\ \phi_4 &= \frac{a^2 \mp 2b}{y^2} + \dots \\ \phi_6 &= \frac{\mp 2ab}{y^3} + \dots \\ \tilde{\phi} &= \frac{b}{y^2} + \dots\end{aligned}\tag{12}$$

with the top sign for the red and the lower sign for the blue puncture. So the pole structure for these punctures is $\{1, 2, 3; 2\}$, with constraints $c_2^{(4)} \pm 2\tilde{c}_2 = \frac{1}{4}(c_1^{(2)})^2$ and $c_3^{(6)} = \mp \tilde{c}_2 c_1^{(2)}$. The \mathbb{Z}_2 outer automorphism acts as $b \mapsto -b$, and it exchanges the red and blue constraints.

¹At red/blue irregular punctures, the convention is reversed. At a red irregular puncture, the constraint is of the form

$$c_l^{(N)} - 2\tilde{c}_l = \dots$$

while, at the corresponding blue irregular puncture, the constraint is

$$c_l^{(N)} + 2\tilde{c}_l = \dots$$

In the presence of red/blue punctures, a little extra care must be taken in computing the graded Coulomb branch dimensions. Too large an excess, of one or the other, over-constrains the differentials and would lead to a difference between the virtual and actual dimension of the Coulomb branch. The dimension of the degree- N component,

$$\dim(V_N) = d_N + \tilde{d} - n_r - n_b \quad (13)$$


where d_N and \tilde{d} are the dimensions we would obtain from applying Riemann-Roch (suitably-adjusted for the other constraints) to ϕ_N and $\tilde{\phi}$, and $n_{r,b}$ are the number of constraints of the form (10), (11) respectively. In order that the constraints not be over-determined, it suffices to ensure that either

$$d_N - n_r \geq 0, \quad \tilde{d} - n_b \geq 0 \quad (14)$$

or

$$d_N - n_b \geq 0, \quad \tilde{d} - n_r \geq 0 \quad (15)$$

holds. Either condition is sufficient to ensure that $\dim(V_N) \geq 0$, but is slightly stronger.


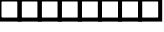
For instance, there is no 3-punctured sphere with three  punctures. The constraints would overconstrain (imply a negative virtual dimension for) the space of sections of the differential $\phi^{(4)} + 2\tilde{\phi}$.

2.2. Irregular Punctures

In addition to regular punctures, we will, again, need to introduce a class of “irregular” punctures, which admit higher-order poles. Ignoring, for the moment, the question of constraints, the class of irregular punctures is the one we introduced in [1] for the A_{N-1} series.

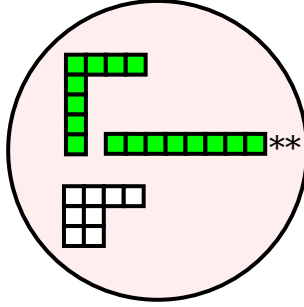
- Each irregular puncture is associated to a simple subgroup $G \subset Spin(2N)$.
- From the pole structure $\{p_k\}$, of the irregular puncture, we construct the “conjugate pole structure,” $\{p'_k\}$
 - $p'_k = p_k = k - 1$ if k is an exponent of G .
 - $p'_k + p_k = 2k - 1$ otherwise.
- We demand that the conjugate pole structure be that of a regular puncture, and we denote the irregular puncture, thus constructed, by the Young diagram of the conjugate regular puncture, with one or more “*”s appended.

Incorporating the constraints simply amounts to “correcting” which values of k correspond to exponents of G .

For example, the D_4 puncture, *, has as its conjugate puncture the maximal puncture, . Its pole structure, $\{1, 3, 5; 4\}$, allows for a quartic, rather than merely a cubic pole for $\tilde{\phi}$. Thus, the corresponding symmetry group is a $Spin(7)$ subgroup

of $Spin(8)$. There are three inequivalent embeddings of $Spin(7) \hookrightarrow Spin(8)$ (depending on which eight-dimensional representation decomposes as the $7 + 1$). Thus, we also have $\color{red}{\blacksquare\blacksquare\blacksquare\blacksquare\blacksquare\blacksquare\blacksquare\blacksquare}^*$ and $\color{blue}{\blacksquare\blacksquare\blacksquare\blacksquare\blacksquare\blacksquare\blacksquare\blacksquare}^*$, which are exchanged by the usual \mathbb{Z}_2 outer automorphism. These latter have pole structure $\{1, 4, 5; 4\}$, and impose, respectively, a constraint $c_4^{(4)} \mp 2\tilde{c}_4 = 0$. This constraint is consequence of using $\phi^{(4)}, \tilde{\phi}$ as our basis of 4-differentials (rather than the linear combination that appears more naturally at a red/blue puncture).

Similarly, the puncture $\color{green}{\blacksquare\blacksquare\blacksquare\blacksquare\blacksquare\blacksquare\blacksquare\blacksquare}^{**}$ corresponds to an $SU(4)$ subgroup of $Spin(8)$, and has poles $\{1, 3, 6; 4\}$. There are again blue and red versions of this puncture corresponding to the other two embeddings of $SU(4)$ related by triality to the green one. The exponent 3 in $SU(4)$ (as opposed to 6) means that we need a constraint $c_6^{(6)} = -(a^{(3)})^2$ that appropriately corrects the dimensions of the Coulomb branch. In a free-field fixture, e.g.,



the constraint $c_6^{(6)} = -(a^{(3)})^2$ from $\color{green}{\blacksquare\blacksquare\blacksquare\blacksquare\blacksquare\blacksquare\blacksquare\blacksquare}^{**}$ offsets the constraint $c_6^{(6)} = (a^{(3)})^2$ from $\color{white}{\blacksquare\blacksquare\blacksquare\blacksquare\blacksquare\blacksquare}$, so the virtual dimension of the Coulomb branch is indeed equal to its actual dimension (zero).

The red and blue versions of this puncture, $\color{red}{\blacksquare\blacksquare\blacksquare\blacksquare\blacksquare\blacksquare\blacksquare\blacksquare}^{**}$ and $\color{blue}{\blacksquare\blacksquare\blacksquare\blacksquare\blacksquare\blacksquare\blacksquare\blacksquare}^{**}$, have poles $\{1, 4, 6; 4\}$, and have the same constraint as the green one, $c_6^{(6)} = -(a^{(3)})^2$, plus an additional constraint $c_4^{(4)} \mp 2\tilde{c}_4 = 0$ as usual.

Finally, we can assign a level, k , to the G symmetry of the irregular puncture. It is simply defined such that the G gauge group on the cylinder, $p \xleftarrow{G} p' \xrightarrow{G}$ between p and its conjugate regular puncture p' , is conformal.

2.3. Central charges

The conformal-anomaly coefficients, a and c , defined via the trace anomaly in a curved background [21],

$$T_\mu{}^\mu = \frac{c}{16\pi^2}(\text{Weyl})^2 - \frac{a}{16\pi^2}(\text{Euler}), \quad (16)$$

are useful invariants, characterizing 4D conformal field theories. Along with the flavour current-algebra central charges [12], k_i , they are among the few readily computable invariants of interacting SCFTs. For the $\mathcal{N} = 2$ SCFTs, under discussion, these invariants are constant [22] over the whole family of SCFTs parametrized by $\mathcal{M}_{g,n}$.

The central charge, k , for each simple factor in the flavour symmetry group associated to a regular puncture can be computed directly from the Young diagram. Denote the length of

the i^{th} row by r_i . In the A_{N-1} case, the flavour symmetry group was given by (4) and each $SU(r_i - r_{i+1})$ factor had level

$$k = 2 \sum_{j=1}^i r_j \quad (17)$$

For the D_N case, the flavour symmetry group is given by (6), and

- For i odd, this gives a $Spin(r_i - r_{i+1})_k$ factor in the flavour symmetry group, where

$$k = \begin{cases} 2 \left(\sum_{j=1}^i r_j \right) - 4 & r_i - r_{i+1} \geq 4 \\ 4 \left(\sum_{j=1}^i r_j \right) - 8 & r_i - r_{i+1} = 3 \end{cases} \quad (18a)$$

- For i even, this gives an $Sp\left(\frac{r_i - r_{i+1}}{2}\right)_k$ in the flavour symmetry group, where

$$k = \sum_{j=1}^i r_j \quad (18b)$$

From Theorem 1, a non-special puncture corresponds to a $2N$ -box Young diagram, whose columns form a D-partition, with at least one (in fact, at least two) odd-length row(s) which appears with odd multiplicity. With a little more work, one can show that at least one of these rows is an even-numbered row. By (18b), this gives an $Sp(l)_k$ factor, in the flavour symmetry group, with k odd. As mentioned in the introduction, this poses an obstruction to gauging: without additional matter to cancel the anomaly, the $Sp(l)$ gauge theory would suffer from Witten's global anomaly [16].

The trace anomaly coefficients, a and c , of the SCFT, can be computed (as we did [1], for the A_{N-1} series) from two auxiliary quantities: the effective number of hypermultiplets, n_h , and the effective number of vector multiplets, n_v ,

$$\begin{aligned} a &= \frac{5n_v + n_h}{24} \\ c &= \frac{2n_v + n_h}{12}. \end{aligned} \quad (19)$$

In [1] we gave formulæ to compute n_h and n_v for regular and irregular punctures in the A_{N-1} series. As before, n_h and n_v are the actual number of hypermultiplets and vector multiplets in a *Lagrangian* S-duality frame of the theory, provided such frame exists. As a consequence, the n_h of a free-field fixture (for which $n_v = 0$) is equal to the number of free hypermultiplets in this fixture.

To compute n_v for a D_N theory on a curve of genus g , one should first calculate the graded dimensions of the Coulomb branch. Then

$$\begin{aligned} n_v &= \sum_k (2k - 1) d_k \\ &= \sum_{k=1}^{N-1} (4k - 1) d_{2k} + \sum_{k=1}^{\lfloor \frac{N-1}{2} \rfloor} (4k + 1) d_{2k+1}. \end{aligned} \quad (20)$$

For example, in the D_4 theory, the possible non-zero Coulomb branch dimensions are d_2, d_3, d_4, d_6 , while in the D_5 theory, they are $d_2, d_3, d_4, d_5, d_6, d_8$. The odd-degree components of the Coulomb branch of the D_N theory appear only up to degree $2[\frac{N-1}{2}] + 1$. We will discuss below how to compute the d_{2k} and d_{2k+1} , but we will treat the case of d_N separately, since it involves the pole orders of the Pfaffian $\tilde{\phi}$.

As we saw before, the even-degree sectors of the Coulomb branch, with dimensions d_{2k} ($2k \neq N$), arise from $2k$ -differentials, and so

$$d_{2k} = (1 - 4k)(1 - g) + \sum_{\alpha} (p_{2k}^{\alpha} - s_{2k}^{\alpha} + t_{2k}^{\alpha}) \quad (21)$$

where α runs over the punctures on the curve, p_{2k}^{α} is the pole order of ϕ_{2k} at the α^{th} puncture, s_{2k}^{α} is the number of constraints of homogeneous degree $2k$ (i.e., polynomial constraints of the form $c_l^{(2k)} = \dots$), and t_{2k}^{α} is the number of $a^{(2k)}$ parameters (i.e., parameters arising from constraints of the form $c_l^{(4k)} = (a^{(2k)})^2$) that the α^{th} puncture contributes.

On the other hand, since there are no ϕ_{2k+1} differentials (except for the Pfaffian, when N is odd), these odd-degree sectors of the Coulomb branch receive contributions *only* from the $a^{(2k+1)}$ parameters (i.e., parameters arising from constraints of the form $c_l^{(4k+2)} = (a^{(2k+1)})^2$). We write

$$d_{2k+1} = \sum_{\alpha} t_{2k+1}^{\alpha}, \quad (22)$$

Notice that this expression is independent of the genus (in contrast to the contributions, to the d_{2k} , from the Riemann-Roch Theorem).

As for d_N , if N is even, then d_N gets a contribution from both ϕ_N and from the Pfaffian $\tilde{\phi}$. The formula for d_N is almost the same as for the d_{2k} case,

$$d_N = 2(1 - 2N)(1 - g) + \sum_{\alpha} (p_N^{\alpha} - s_N^{\alpha}) + \tilde{p}^{\alpha}. \quad (23)$$

Notice that there is no t_N^{α} term, since we do not have a $2N$ -differential.

Similarly, if N is odd, only the Pfaffian (the unique odd-degree differential) contributes to d_N , and so,

$$d_N = (1 - 2N)(1 - g) + \sum_{\alpha} \tilde{p}^{\alpha}. \quad (24)$$

Adding up the global, genus-dependent contribution from the $2k$ -differentials and the Pfaffian, we obtain


$$n_v = -\frac{1}{3}(1 - g)N(16N^2 - 24N + 11) + \sum_{\alpha} \delta n_v^{(\alpha)}, \quad (25)$$

where α runs over the punctures on the curve, and the contribution $\delta n_v^{(\alpha)}$ of the α^{th} puncture to n_v is

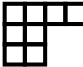
$$\delta n_v^{(\alpha)} = \sum_{k=1}^{N-1} (4k-1)(p_{2k}^\alpha - s_{2k}^\alpha + t_{2k}^\alpha) + \sum_{k=1}^{\lfloor \frac{N-1}{2} \rfloor} (4k+1)t_{2k+1}^\alpha + (2N-1)\tilde{p}^\alpha \quad (26)$$

Let us see a few examples of how to compute δn_v . First, consider the maximal D_3 puncture, which has poles $\{1, 3; 2\}$, and no constraints. One gets


$$\delta n_v = 3(1) + 7(3) + 5(2) = 34. \quad (27)$$

Next, consider the D_4 puncture, . The poles are $\{1, 3, 4; 3\}$ and there is one constraint ($c_3^{(4)} + 2\tilde{c}_3 = 0$), so $s_4 = 1$. We then have

$$\delta n_v = 3(1) + 7(3-1) + 11(4) + 7(3) = 82. \quad (28)$$

Now consider the D_4 puncture . The poles are $\{1, 2, 4; 2\}$ and there is one constraint ($c_4^{(6)} = (a^{(3)})^2$), so $s_6 = 1$ and $t_3 = 1$. Thus,

$$\delta n_v = 3(1) + 7(2) + 11(4-1) + 7(2) + 5(1) = 69. \quad (29)$$

Now look at the non-special D_4 puncture . Its poles are $\{1, 2, 4; 2\}$, and it has no constraints. This means that

$$\delta n_v = 3(1) + 7(2) + 11(4) + 7(2) = 75. \quad (30)$$

Finally, let us look at the D_5 puncture

$$\begin{array}{|c|c|c|c|} \hline \square & \square & \square & \square \\ \hline \square & \square & \square & \square \\ \hline \square & \square & \square & \square \\ \hline \square & \square & \square & \square \\ \hline \end{array} \quad (31)$$

which has poles $\{1, 2, 4, 5; 3\}$. The two constraints ($c_4^{(6)} = (a^{(3)})^2$ and $c_5^{(8)} = 2a^{(3)}\tilde{c}_3$) imply that $t_6 = 1$, $t_8 = 1$, and $s_3 = 1$. Hence,

$$\delta n_v = 3(1) + 7(2) + 11(4-1) + 15(5-1) + 9(3) + 5(1) = 142. \quad (32)$$

Let us now go on to discuss n_h . Just like n_v , n_h is a sum of a global piece and contributions from each puncture,

$$n_h = -\frac{8}{3}(1-g)N(N-1)(2N-1) + \sum_{\alpha} \delta n_h^{(\alpha)} \quad (33)$$

where α runs over the punctures, and

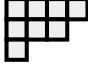
$$\delta n_h^{(\alpha)} = \delta n_v^{(\alpha)} + f^{(\alpha)} \quad (34)$$

is the contribution of the α^{th} puncture to n_h . We will see below how to compute $f^{(\alpha)}$ for regular and irregular punctures.

For a *regular* puncture, $f^{(\alpha)}$ can be found from the row-lengths $r_1 \geq r_2 \geq \dots$ of the flavour Young diagram,

$$f^{(reg)} = \frac{1}{4} \sum r_i^2 - \frac{1}{2} \sum r_{odd}, \quad (35)$$

where the first sum is over all rows, and the second is restricted to odd-numbered rows ($r_1, r_3, r_5, r_7, \dots$).

For example, the D_4 puncture, , has $f = \frac{1}{4}[4^2 + 3^2 + 1^2] - \frac{1}{2}[4 + 1] = 4$. Since we previously computed $n_v = 75$ for this puncture, we have $n_h = 79$.

The $f^{(irreg)}$ for an irregular puncture, p , follows from consistency with degeneration,

$$f^{(irreg)} = -N + \dim G - f^{(reg)}, \quad (36)$$

where $f^{(reg)}$ is the contribution of the regular puncture, p' , conjugate to p . G is the flavour symmetry group we ascribe to the irregular puncture, p (equivalently, the gauge group on the cylinder $p \xleftarrow{G} p' \rightarrow p$).

2.4. Regular Punctures (up through D_6)




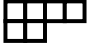
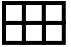
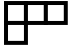
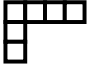
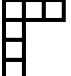

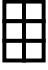


We list below the properties of regular punctures for D_3 , D_4 , D_5 , and D_6 . In writing down the global symmetry groups, it will be convenient to use the isomorphisms

$$\begin{aligned} Spin(2) &\simeq U(1) \\ Spin(3) &\simeq Sp(1) \simeq SU(2) \\ Spin(4) &\simeq SU(2)^2 \\ Spin(5) &\simeq Sp(2) \\ Spin(6) &\simeq SU(4) \end{aligned} \quad (37)$$

As in the A_{N-1} case, there's a Young diagram (this time, with a column of height $2N-1$ and a column of height 1), which corresponds to a regular point on the curve C , so we exclude it from our discussion.

2.4.1. D_3

Since $D_3 \simeq A_3$, the results for D_3 were already reported in our previous paper. However, as a warm-up, it will be convenient to repeat them here, recast in the notation we will use for the higher entries in the D_N series.

Young Diagram	Nilpotent Orbit	Pole structure	Constraints	A_3 Young Diagram	Flavour Symmetry	$(\delta n_h, \delta n_v)$
		$\{1, 3; 2\}$	—		$SU(4)_8$	$(40, 34)$
		$\{1, 2; 2\}$	—		$SU(2)_6 \times U(1)$	$(30, 27)$
		$\{1, 2; 1\}$	—		$SU(2)_8$	$(24, 22)$
		$\{1, 2; 1\}$	$c_2^{(4)} = \frac{1}{4} \left(c_1^{(2)} \right)^2$		$U(1)$	$(16, 15)$

Note that, in the D_3 description, the quartic differential is allowed to have a double pole at the minimal puncture, instead of only a simple pole (as in the A_3 description). However, the coefficient of the double pole is constrained, so that the Coulomb branch has the same graded dimension as before.

2.4.2. D_4

For D_4 , the outer automorphism group is enhanced from \mathbb{Z}_2 to S_3 . Hence, the pairs of punctures, which were related by exchanging $8_s \leftrightarrow 8_c$, are actually organized into triples, under permutations of $8_s, 8_c, 8_v$. We indicate this by colouring the Young diagram, corresponding to the other puncture in the triple, green.

The fact that the nilpotent orbits in a triple are related by triality becomes particularly clear if one looks at their weighted Dynkin diagrams ([15]). More practical evidence comes from the fact that the punctures in a triple exhibit the same flavour group and $(\delta n_h, \delta n_v)$.

In this table, and in the D_5 , D_6 tables below, we've shaded each non-special flavour Young diagram and the (special) nilpotent orbit which is its image under the Spaltenstein map.

Young Diagram	Nilpotent orbit	Pole structure	Constraints	Flavour Symmetry	$(\delta n_h, \delta n_v)$
		$\{1, 3, 5; 3\}$	—	$Spin(8)_{12}$	$(112, 100)$
		$\{1, 3, 4; 3\}$	—	$SU(2)_8^3$	$(96, 89)$
		$\{1, 3, 4; 2\}$	—	$Sp(2)_8$	$(88, 82)$
		$\{1, 3, 4; 3\}$	$c_3^{(4)} \pm 2\tilde{c}_3 = 0$	$Sp(2)_8$	$(88, 82)$
		$\{1, 2, 4; 2\}$	$c_4^{(6)} = (a^{(3)})^2$	$U(1)^2$	$(72, 69)$
	—	$\{1, 2, 4; 2\}$	—	$SU(2)_7$	$(79, 75)$
		$\{1, 2, 2; 1\}$	—	$SU(2)_8$	$(48, 46)$
		$\{1, 2, 3; 2\}$	$c_2^{(4)} \pm 2\tilde{c}_2 = \frac{1}{4} (c_1^{(2)})^2$ $c_3^{(6)} = \mp \tilde{c}_2 c_1^{(2)}$	$SU(2)_8$	$(48, 46)$
		$\{1, 2, 2; 1\}$	$c_2^{(4)} = \frac{1}{4} (c_1^{(2)})^2$	none	$(40, 39)$

2.4.3. D_5

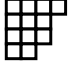
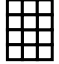
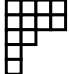

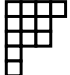
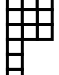
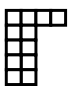
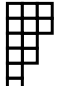
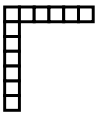
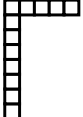

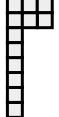
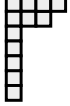
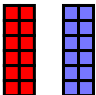
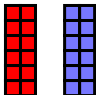
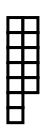


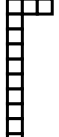


Young Diagram	Nilpotent Orbit	Pole structure	Constraints	Flavour Symmetry	$(\delta n_h, \delta n_v)$
		$\{1, 3, 5, 7; 4\}$	—	$Spin(10)_{16}$	$(240, 220)$

		$\{1, 3, 5, 6; 4\}$	—	$SU(4)_{12} \times SU(2)_{10}$	(218, 205)
		$\{1, 3, 5, 6; 3\}$	—	$Spin(7)_{12}$	(208, 196)
		$\{1, 3, 4, 6; 4\}$	—	$Sp(2)_{10} \times U(1)$	(204, 194)
		$\{1, 3, 4, 6; 3\}$	$c_6^{(8)} = (a^{(4)})^2$	$SU(2)_8^2 \times U(1)$	(184, 177)
	—	$\{1, 3, 4, 6; 3\}$	—	$SU(2)_{16} \times SU(2)_9$	(193, 185)
		$\{1, 3, 4, 6; 3\}$	$c_6^{(8)} = \frac{1}{4} (c_3^{(4)})^2$	$SU(2)_8 \times U(1)$	(176, 170)
		$\{1, 2, 4, 5; 3\}$	—	$SU(2)_{32}$	(168, 163)
		$\{1, 3, 4, 4; 2\}$	—	$Sp(2)_8$	(152, 146)
		$\{1, 2, 4, 5; 3\}$	$c_4^{(6)} = (a^{(3)})^2$ $c_5^{(8)} = 2a^{(3)}\tilde{c}_3$	$SU(2)_{10} \times U(1)$	(146, 142)
		$\{1, 2, 4, 4; 2\}$	$c_4^{(6)} = (a^{(3)})^2$	$U(1)$	(136, 133)
	—	$\{1, 2, 4, 4; 2\}$	—	$SU(2)_7$	(143, 139)
		$\{1, 2, 3, 4; 2\}$	$c_3^{(6)} = \frac{1}{2} c_1^{(2)} \left(c_2^{(4)} - \frac{1}{4} (c_1^{(2)})^2 \right)$ $c_4^{(8)} = \frac{1}{4} \left(c_2^{(4)} - \frac{1}{4} (c_1^{(2)})^2 \right)^2$	$U(1)$	(104, 102)
		$\{1, 2, 2, 2; 1\}$	—	$SU(2)_8$	(80, 78)
		$\{1, 2, 2, 2; 1\}$	$c_2^{(4)} = \frac{1}{4} (c_1^{(2)})^2$	<i>none</i>	(72, 71)

2.4.4. D_6

Again, in D_6 , we have very-even partitions, which correspond to two *distinct* punctures, which we have coloured red and blue.


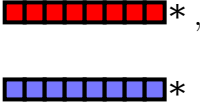

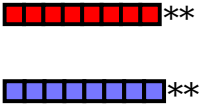

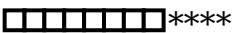


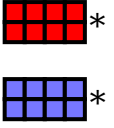

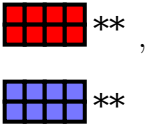

Young Diagram	Nilpotent orbit	Pole structure	Constraints	Flavour Symmetry	$(\delta n_h, \delta n_v)$
		$\{1, 3, 5, 7, 9; 5\}$	—	$Spin(12)_{20}$	(440, 410)
		$\{1, 3, 5, 7, 8; 5\}$	—	$Spin(8)_{16} \times SU(2)_{12}$	(412, 391)
		$\{1, 3, 5, 7, 8; 4\}$	—	$Spin(9)_{16}$	(400, 380)
		$\{1, 3, 5, 6, 8; 5\}$	—	$Sp(2)_{12} \times SU(2)_{12}^2$	(392, 376)
		$\{1, 3, 5, 6, 8; 5\}$	$c_5^{(6)} \pm 2\tilde{c}_5 = 0$	$Sp(3)_{12}$	(380, 365)
		$\{1, 3, 5, 6, 8; 4\}$	$c_8^{(10)} = (a^{(5)})^2$	$SU(4)_{12} \times U(1)$	(368, 355)
	—	$\{1, 3, 5, 6, 8; 4\}$	—	$Sp(2)_{12} \times SU(2)_{11}$	(379, 365)
		$\{1, 3, 4, 6, 8; 4\}$	$c_8^{(10)} = (a^{(5)})^2$	$SU(2)_{10} \times U(1)^2$	(354, 344)
	—	$\{1, 3, 4, 6, 8; 4\}$	—	$Sp(2)_{11}$	(366, 354)
		$\{1, 3, 4, 6, 7; 4\}$	—	$SU(2)_{40} \times SU(2)_{16}$	(344, 335)
		$\{1, 3, 4, 6, 7; 4\}$	$c_6^{(8)} = \frac{1}{4}(c_3^{(4)})^2$	$SU(2)_{20}^2$	(328, 320)
		$\{1, 3, 5, 6, 6; 3\}$	—	$Spin(7)_{12}$	(328, 316)
		$\{1, 3, 4, 6, 7; 4\}$	$c_6^{(8)} = (a^{(4)})^2$ $c_7^{(10)} = a^{(4)}\tilde{c}_4$	$SU(2)_{12} \times SU(2)_8^2$	(316, 308)
		$\{1, 3, 4, 6, 7; 4\}$	$c_6^{(8)} = \frac{1}{4}(c_3^{(4)})^2$ $c_7^{(10)} = \pm \tilde{c}_4 c_3^{(4)}$	$SU(2)_{12} \times SU(2)_8$	(308, 301)
		$\{1, 3, 4, 6, 6; 3\}$	$c_6^{(8)} = (a^{(4)})^2$	$SU(2)_8^2$	(304, 297)
	—	$\{1, 3, 4, 6, 6; 3\}$	—	$SU(2)_{16} \times SU(2)_9$	(313, 305)

		$\{1, 2, 4, 5, 6; 4\}$	—	$SU(2)_{12}$	(300, 294)
		$\{1, 3, 4, 6, 6; 3\}$	$c_6^{(8)} = \frac{1}{4}(c_3^{(4)})^2$	$SU(2)_8$	(296, 290)
		$\{1, 2, 4, 5, 6; 3\}$	—	$U(1)$	(288, 283)
		$\{1, 2, 4, 5, 6; 3\}$	$c_4^{(6)} = (a^{(3)})^2$ $c_6^{(10)} = (a^{(5)})^2$ $c_4^{(8)} = 2a^{(3)}a^{(5)}$	$U(1)^2$	(256, 252)
		$\{1, 3, 4, 4, 4; 2\}$	—	$Sp(2)_8$	(232, 226)
		$\{1, 2, 4, 4, 4; 2\}$	$c_4^{(6)} = (a^{(3)})^2$	$U(1)$	(216, 213)
	—	$\{1, 2, 4, 4, 4; 2\}$	—	$SU(2)_7$	(223, 219)
		$\{1, 2, 3, 4, 5; 3\}$	$c_3^{(6)} \pm 2\tilde{c}_3 = \frac{1}{2}c_1^{(2)} \left(c_2^{(4)} - \frac{1}{3}(c_1^{(2)})^2 \right)$ $c_4^{(8)} = \frac{1}{4} \left(c_2^{(4)} - \frac{1}{3}(c_1^{(2)})^2 \right)^2 \mp \tilde{c}_3 c_1^{(2)}$ $c_5^{(10)} = \mp \tilde{c}_3 \left(c_2^{(4)} - \frac{1}{3}(c_1^{(2)})^2 \right)$	$SU(2)_{12}$	(196, 193)
		$\{1, 2, 3, 4, 4; 2\}$	$c_3^{(6)} = \frac{1}{2}c_1^{(2)} \left(c_2^{(4)} - \frac{1}{3}(c_1^{(2)})^2 \right)$ $c_4^{(8)} = \frac{1}{4} \left(c_2^{(4)} - \frac{1}{3}(c_1^{(2)})^2 \right)^2$	none	(184, 182)
		$\{1, 2, 2, 2, 2; 1\}$	—	$SU(2)_8$	(120, 118)
		$\{1, 2, 2, 2, 2; 1\}$	$c_2^{(4)} = \frac{1}{4}(c_1^{(2)})^2$	none	(112, 111)

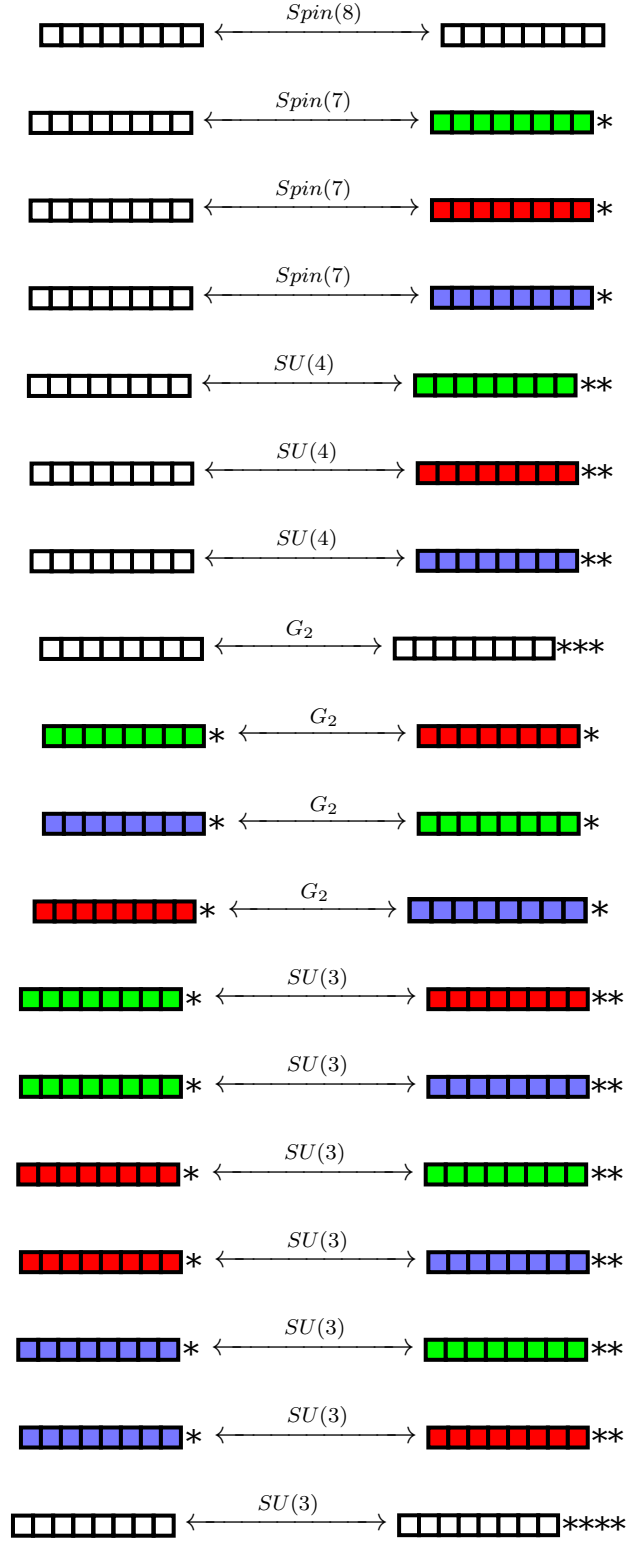
3. The D_4 theory

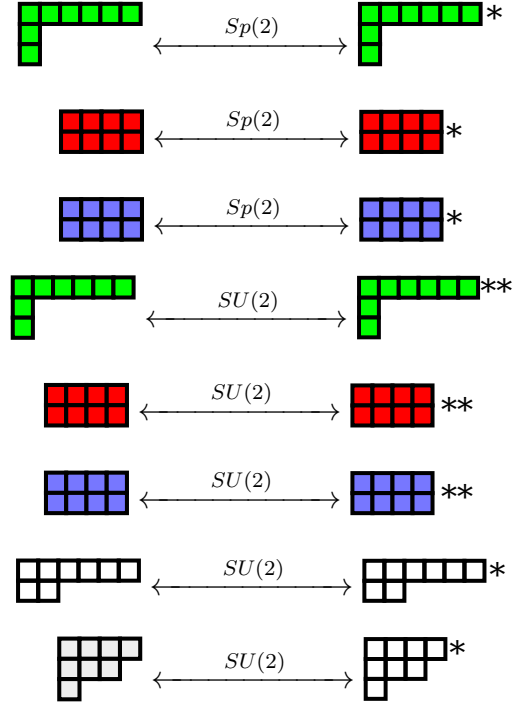
3.1. Irregular punctures and cylinders

In this section, we will develop the complete “tinkertoy” catalogue for the D_4 theory. The regular punctures are listed in §2.4.2. In the D_4 case, we have the following list of irregular punctures.

Young Diagram	Pole structure	Constraints	Flavour Symmetry	$(\delta n_h, \delta n_v)$
	$\{1, 3, 5; 4\}$	—	$Spin(7)_8$	$(112, 107)$
	$\{1, 4, 5; 4\}$	$c_4^{(4)} \mp 2\tilde{c}_4 = 0$	$Spin(7)_8$	$(112, 107)$
	$\{1, 3, 6; 4\}$	$c_6^{(6)} = -(a^{(3)})^2$	$SU(4)_4$	$(112, 113)$
	$\{1, 4, 6; 4\}$	$c_4^{(4)} \mp 2\tilde{c}_4 = 0$ $c_6^{(6)} = -(a^{(3)})^2$	$SU(4)_4$	$(112, 113)$
	$\{1, 4, 5; 4\}$	—	$(G_2)_4$	$(112, 114)$
	$\{1, 4, 6; 4\}$	$c_6^{(6)} = -(a^{(3)})^2$	$SU(3)_0$	$(112, 120)$
	$\{1, 4, 7; 4\}$	—	$SU(2)_0$	$(128, 136)$
	$\{1, 3, 7; 5\}$	—	$Sp(2)_4$	$(136, 136)$
	$\{1, 5, 7; 5\}$	$c_5^{(4)} \mp \tilde{c}_5 = 0$ $c_4^{(4)} \mp \tilde{c}_4 = 0$	$Sp(2)_4$	$(136, 136)$
	$\{1, 4, 7; 5\}$	—	$SU(2)_0$	$(136, 143)$
	$\{1, 5, 7; 5\}$	$c_5^{(4)} \mp \tilde{c}_5 = 0$	$SU(2)_0$	$(136, 143)$
	$\{1, 5, 7; 5\}$	—	$SU(2)_1$	$(145, 150)$

The cylinders in the D_4 theory are





Note that some of the irregular punctures have level $k = 0$. Appropriately, these will appear, below, on “empty” fixtures, with zero hypermultiplets. Also, note that each of the cylinders, $p \xleftrightarrow{G} p'$, satisfies

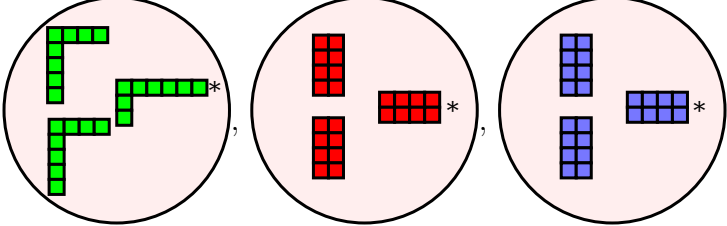
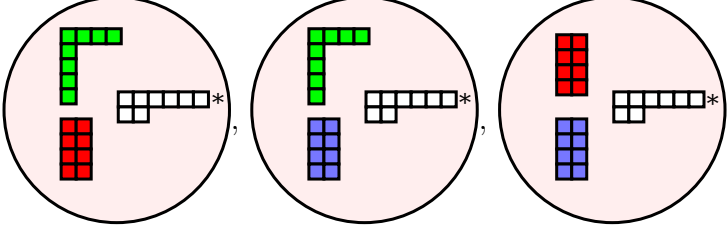
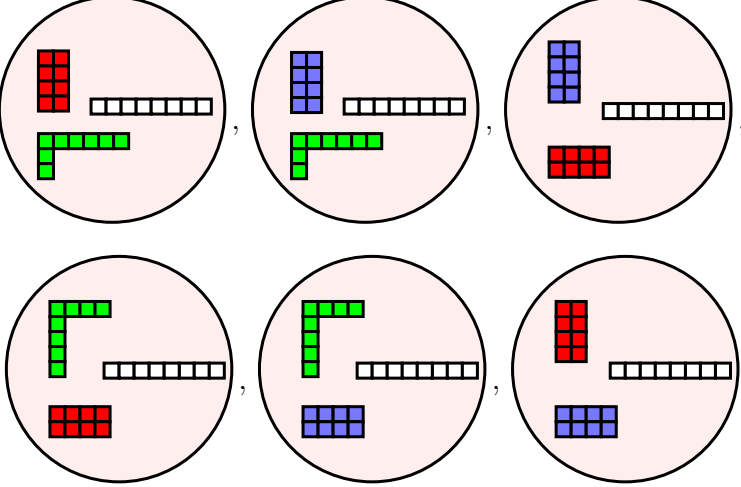
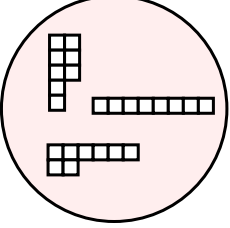
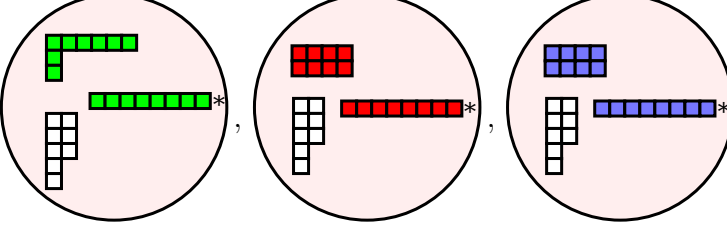
$$\begin{aligned}
 \delta n_h + \delta n_h' - 8N(N-1)(2N-1)/3 &= 0 \\
 \delta n_v + \delta n_v' - N(16N^2 - 24N + 11)/3 &= \dim(G) \\
 k + k' &= k_{\text{critical}}
 \end{aligned} \tag{38}$$

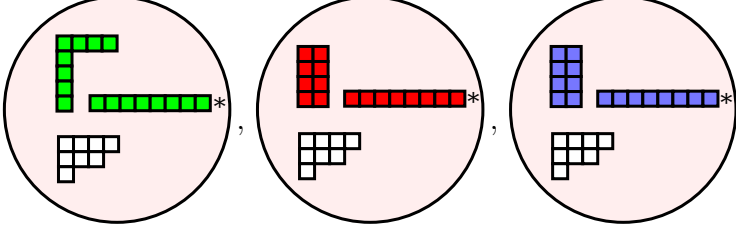
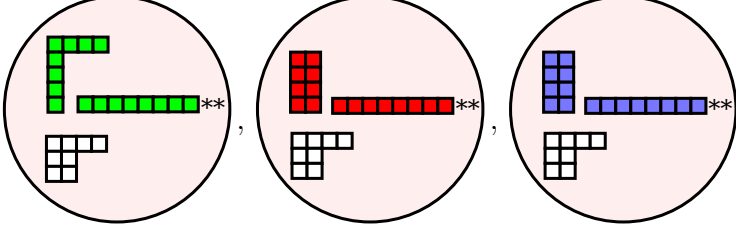
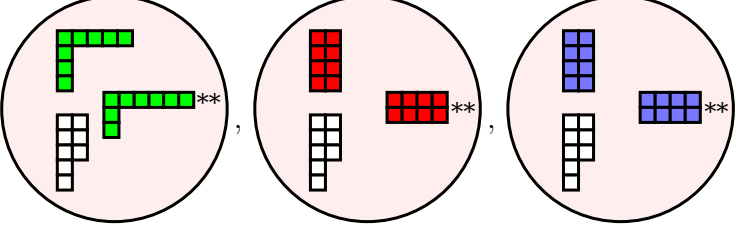
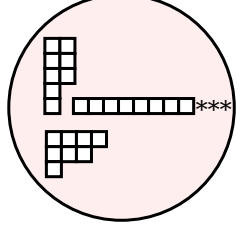
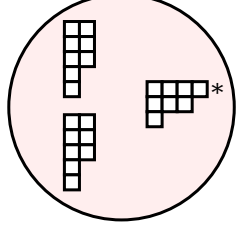
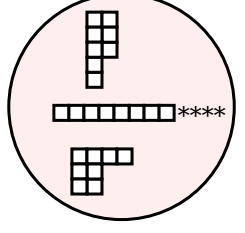
where $k_{\text{critical}} = 2\ell_{\text{adj}}$ is the value of k which gives vanishing β -function for G . While this was true (by construction) when p' is the conjugate regular puncture to p , it's not automatically-satisfied for cylinders between two irregular punctures. In essence, these conditions determine which cylinders between pairs of irregular punctures are allowed.

3.2. Fixtures

Here, we list all of the 3-punctured spheres. There are a lot of them, but fortunately, the profusion is partially tamed by the fact that they are organized into multiplets under the outer automorphism group.

3.2.1. Free-field fixtures

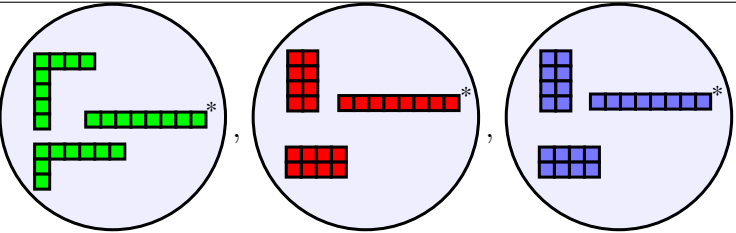
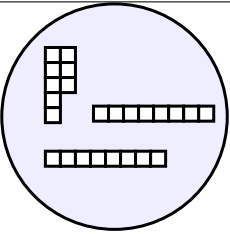
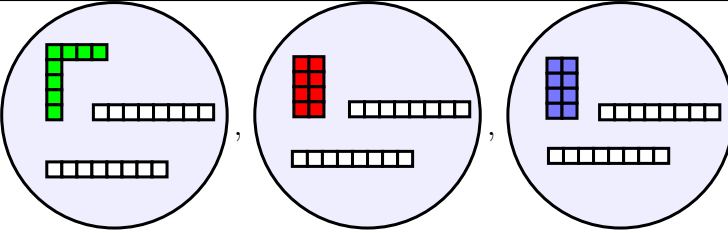
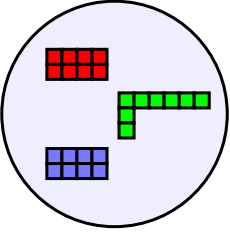
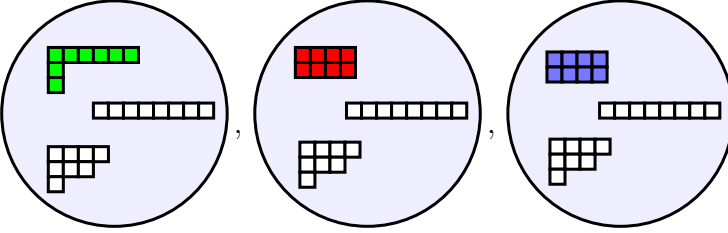
Fixture	Number of Hypers	Representation
	8	$\frac{1}{2}(2, 2, 4)$
	0	none
	24	$\frac{1}{2}(1, 4, 8_u) + \frac{1}{2}(2, 1, 8_d)$, where $8_{u/d} = 8_v, 8_s$, or 8_c depending on whether the upper/lower left-hand puncture is coloured green, red, or blue.
	24	$\frac{1}{2}(2, 1, 1, 8_v)$ $+ \frac{1}{2}(1, 2, 1, 8_s)$ $+ \frac{1}{2}(1, 1, 2, 8_c)$
	16	$\frac{1}{2}(4, 8)$

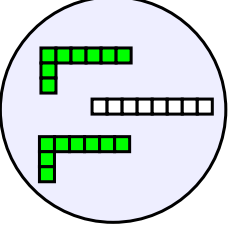
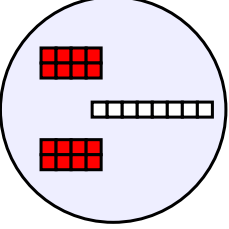
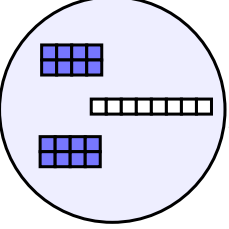
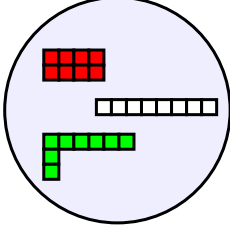
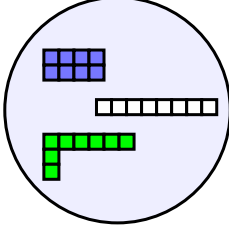
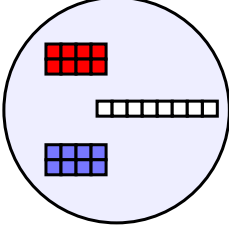
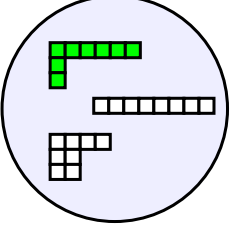
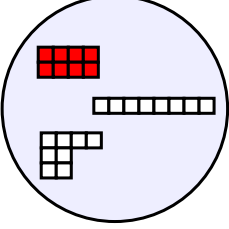
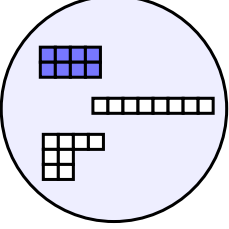
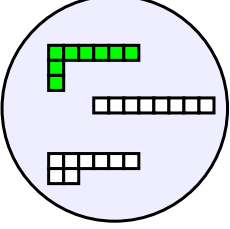
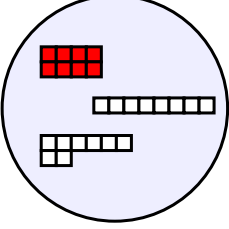
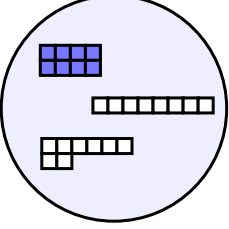
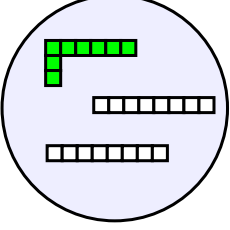
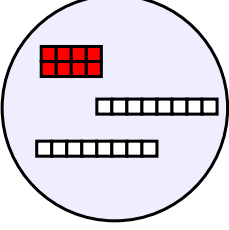
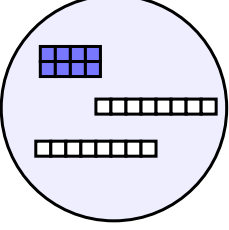
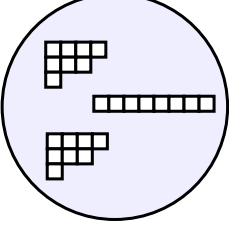
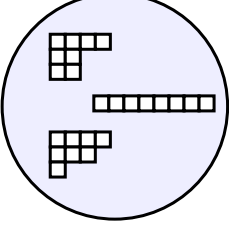
	15	$\frac{1}{2}(2, 1, 8) + \frac{1}{2}(1, 2, 7)$
	8	$(2, 4)$
	0	none
	7	$\frac{1}{2}(2, 7)$
	1	$\frac{1}{2}(2)$
	0	none

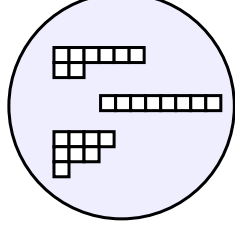
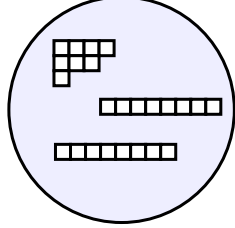
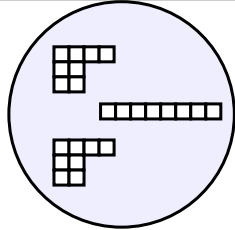
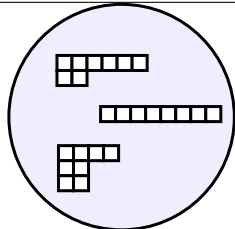
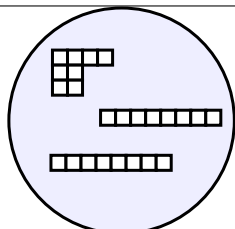
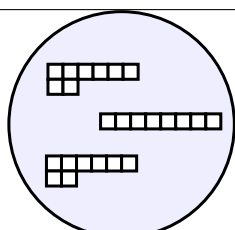
Note that, among the free field fixtures, are six which are empty (zero hypermultiplets). It might, at first blush, seem peculiar to assign global symmetry groups ($SU(2)_8^2$ and $SU(2)_8$, respectively) to the regular punctures on them. However, they are attached to the rest of the surface by an $SU(2)$ cylinder, which gauges an $SU(2)$ subgroup of the global symmetry

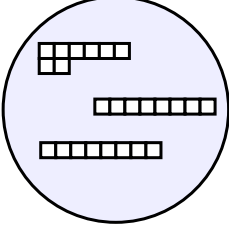
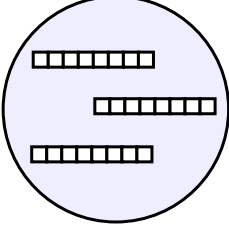
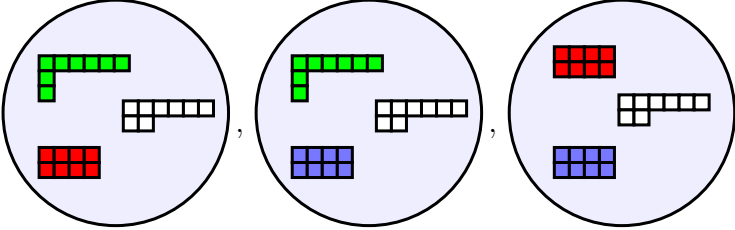
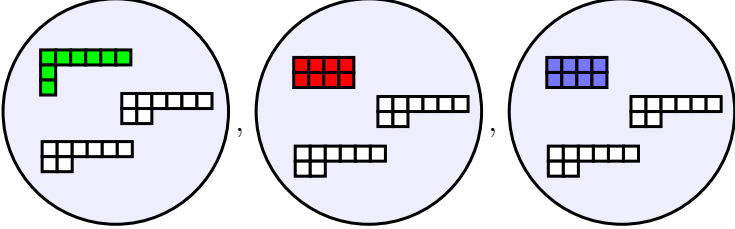
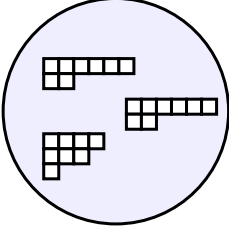
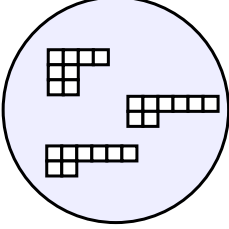
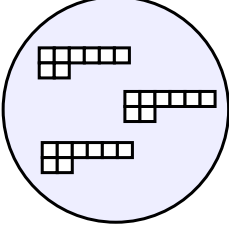
group of the attaching puncture. The centralizer of that $SU(2)$ is, respectively $SU(2)_8^2$ or $SU(2)_8$. That centralizer is what is detected by the punctures on the ostensibly “empty” fixture. Similar remarks applied to the analogous fixtures that we saw in the D_3 and A_{N-1} cases, studied in [1].

3.2.2. Interacting fixtures

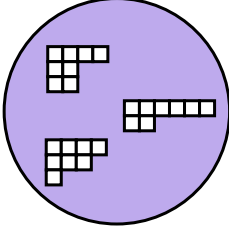
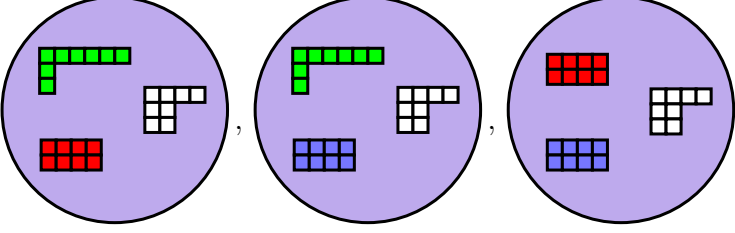
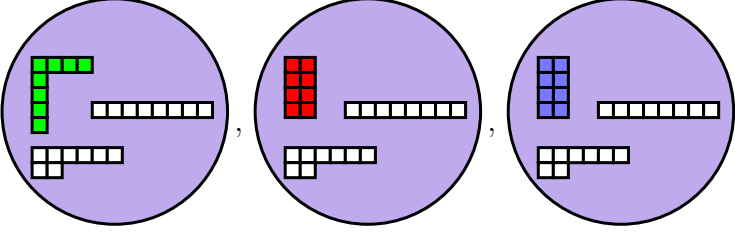
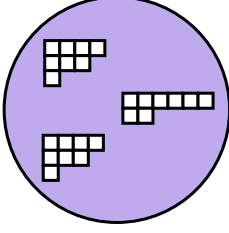
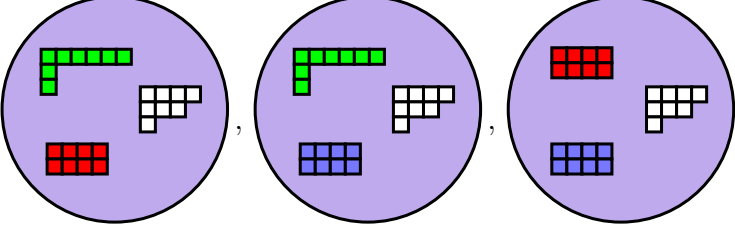
Fixture	$(d_2, d_3, d_4, d_5, d_6)$	(a, c)	$(G_{\text{global}})_k$	Theory
	$(0, 0, 1, 0, 0)$	$(\frac{59}{24}, \frac{19}{6})$	$(E_7)_8$	The E_7 SCFT
	$(0, 0, 0, 0, 1)$	$(\frac{95}{24}, \frac{31}{6})$	$(E_8)_{12}$	The E_8 SCFT
	$(0, 0, 1, 0, 1)$	$(\frac{23}{4}, 7)$	$Spin(8)_{12}^2 \times SU(2)_8$	
	$(0, 0, 1, 0, 1)$	$(\frac{65}{12}, \frac{19}{3})$	$Sp(6)_8$	
	$(0, 0, 1, 0, 2)$	$(\frac{25}{3}, \frac{113}{12})$	$Spin(8)_{12} \times Sp(2)_8 \times SU(2)_7$	

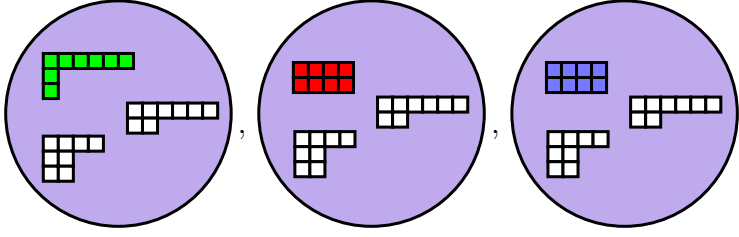
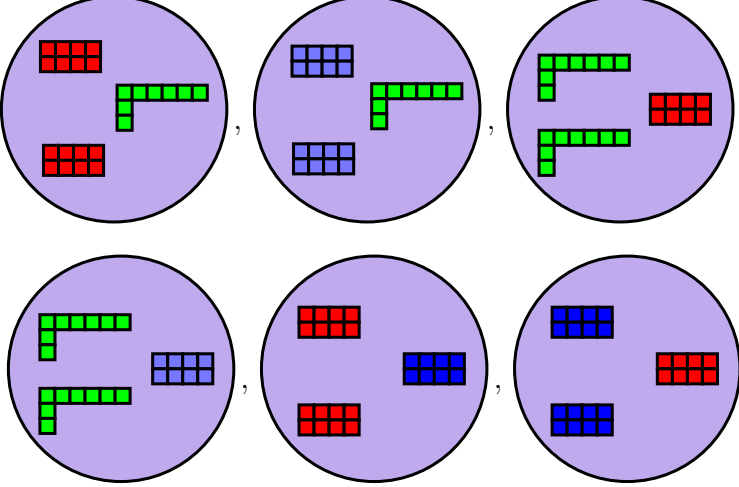
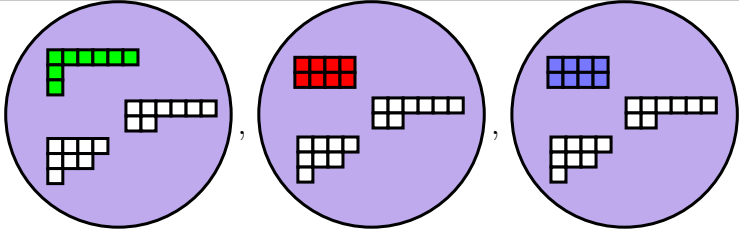
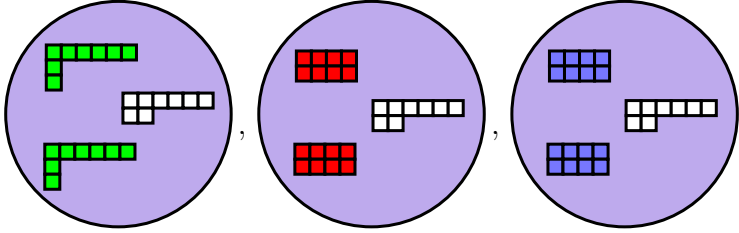
  	$(0, 0, 2, 0, 2)$	$(\frac{61}{6}, \frac{34}{3})$	$Spin(8)_{12} \times Sp(2)_8^2$	
  				
  	$(0, 1, 1, 0, 1)$	$(\frac{163}{24}, \frac{47}{6})$	$Spin(8)_{12} \times Sp(2)_8 \times U(1)^2$	
  	$(0, 0, 3, 0, 2)$	$(\frac{287}{24}, \frac{79}{6})$	$Spin(8)_{12} \times Sp(2)_8 \times SU(2)_8^3$	
  	$(0, 0, 3, 0, 3)$	$(\frac{179}{12}, \frac{49}{3})$	$Spin(8)_{12}^2 \times Sp(2)_8$	
	$(0, 0, 0, 0, 2)$	$(\frac{13}{2}, \frac{15}{2})$	$Spin(8)_{12} \times SU(2)_7^2$	
	$(0, 1, 0, 0, 1)$	$(\frac{119}{24}, \frac{71}{12})$	$Spin(8)_{12} \times SU(2)_7 \times U(1)^2$	

	$(0, 0, 2, 0, 2)$	$(\frac{81}{8}, \frac{45}{4})$	$Spin(8)_{12} \times SU(2)_8^3 \times SU(2)_7$	
	$(0, 0, 2, 0, 3)$	$(\frac{157}{12}, \frac{173}{12})$	$Spin(8)_{12}^2 \times SU(2)_7$	
	$(0, 2, 0, 0, 0)$	$(\frac{41}{12}, \frac{13}{3})$	$Spin(8)_{12} \times U(1)^4$	
	$(0, 1, 2, 0, 1)$	$(\frac{103}{12}, \frac{29}{3})$	$Spin(8)_{12} \times SU(2)_8^3 \times U(1)^2$	
	$(0, 1, 2, 0, 2)$	$(\frac{277}{24}, \frac{77}{6})$	$Spin(8)_{12}^2 \times U(1)^2$	
	$(0, 0, 4, 0, 2)$	$(\frac{55}{4}, 15)$	$Spin(8)_{12} \times SU(2)_8^6$	

	$(0, 0, 4, 0, 3)$	$(\frac{401}{24}, \frac{109}{6})$	$Spin(8)_{12}^2 \times SU(2)_8^3$	
	$(0, 0, 4, 0, 4)$	$(\frac{59}{3}, \frac{64}{3})$	$Spin(8)_{12}^3$	
	$(0, 0, 2, 0, 1)$	$(\frac{173}{24}, \frac{49}{6})$	$Sp(3)_8^2 \times SU(2)_8$	
	$(0, 0, 3, 0, 1)$	$(9, 10)$	$Sp(2)_8^2 \times SU(2)_8^4$	
	$(0, 0, 2, 0, 1)$	$(\frac{43}{6}, \frac{97}{12})$	$Sp(2)_8^3 \times SU(2)_7$	
	$(0, 1, 2, 0, 0)$	$(\frac{45}{8}, \frac{13}{2})$	$SU(4)_8^3$	T_4
	$(0, 0, 4, 0, 1)$	$(\frac{259}{24}, \frac{71}{6})$	$SU(2)_8^9$	

3.2.3. Mixed fixtures

Fixture	$(d_2, d_3, d_4, d_5, d_6)$	(a, c)	SCFT	# Free hypers
	$(0, 1, 0, 0, 0)$	$(2, \frac{11}{4})$	$(E_6)_6$	7 hypers, transforming as $\frac{1}{2}(2; 1, 1, 1)$ $+(1; 2, 1, 1)$ $+(1; 1, 2, 1)$ $+(1; 1, 1, 2)$
	$(0, 1, 0, 0, 0)$	$(\frac{49}{24}, \frac{17}{6})$	$(E_6)_6$	8 hypers, transforming as $(4; 1) + (1; 4)$
	$(0, 0, 1, 0, 0)$	$(\frac{67}{24}, \frac{23}{6})$	$(E_7)_8$	8 hypers, transforming as the $(1; 1, 1, 1; 8_u)$, where $8_u = 8_{v,s,c}$, depending on the colour of the puncture on the upper left
	$(0, 0, 0, 0, 1)$	$(\frac{85}{24}, \frac{13}{3})$	$Sp(5)_7$	3 hypers, transforming as $\frac{1}{2}(1; 1; 2, 1, 1)$ $+\frac{1}{2}(1; 1; 1, 2, 1)$ $+\frac{1}{2}(1; 1; 1, 1, 2)$
	$(0, 0, 0, 0, 1)$	$(\frac{43}{12}, \frac{53}{12})$	$Sp(5)_7$	4 hypers, transforming as $\frac{1}{2}(1; 4; 1)$ $+\frac{1}{2}(4; 1; 1)$

	$(0, 1, 1, 0, 0)$	$(\frac{23}{6}, \frac{14}{3})$	$SU(2)_6 \times SU(8)_8$	2 hypers, transforming as $(1; 2, 1, 1)$
	$(0, 0, 1, 0, 1)$	$(\frac{65}{12}, \frac{19}{3})$	$Sp(4)_8 \times Sp(2)_7$	2 hypers, transforming as $\frac{1}{2}(1; 1; 4)$
	$(0, 0, 1, 0, 1)$	$(\frac{43}{8}, \frac{25}{4})$	$Sp(4)_8 \times Sp(2)_7$	1 hyper, transforming as $\frac{1}{2}(1; 1; 2, 1, 1)$
	$(0, 0, 2, 0, 1)$	$(\frac{173}{24}, \frac{49}{6})$	$Sp(2)_8^3 \times SU(2)_7$	1 hyper, transforming as $\frac{1}{2}(1; 1; 2, 1, 1)$

3.3. The $Sp(4)_8 \times Sp(2)_7$ and $Sp(5)_7$ SCFTs

A couple of SCFTs make a somewhat unusual appearance in the above list of mixed fixtures. Usually, the mixed fixtures contain SCFTs which have previously appeared elsewhere (without the additional hypermultiplets). In the present case, we find two new ones, which do not appear to arise *in the absence* of accompanying hypermultiplets.

3.3.1. $Sp(4)_8 \times Sp(2)_7$ SCFT

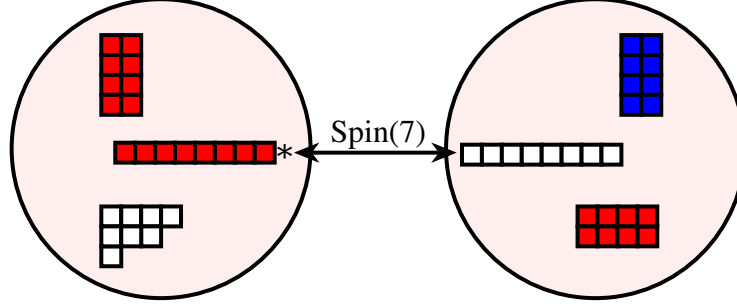
One is the $Sp(4)_8 \times Sp(2)_7$ SCFT. It has $(a, c) = (\frac{16}{3}, \frac{37}{6})$, and graded Coulomb branch dimension $(d_2, d_3, d_4, d_5, d_6) = (0, 0, 1, 0, 1)$. Its global symmetry group is

$$G_X = Sp(4)_8 \times Sp(2)_7$$

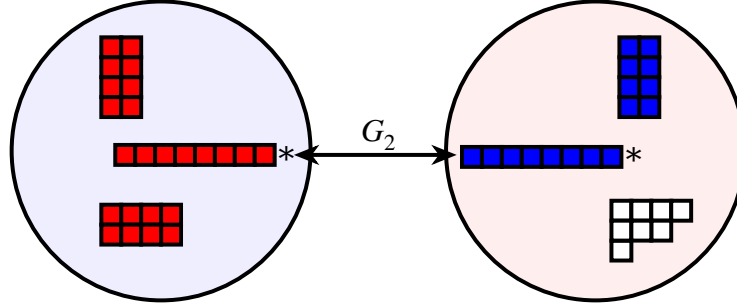
It appears in our table, accompanied by either 1 hypermultiplet (3 fixtures) or 2 hypermultiplets (6 fixtures).

Let's look a couple of examples of its appearance.

Consider a $Spin(7)$ gauge theory, with matter in the $3(8) + 2(7) + 1$.

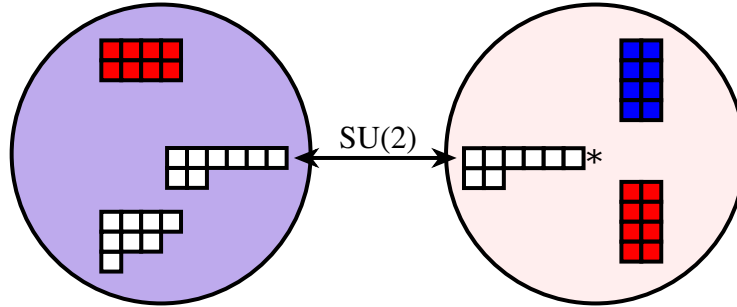


This theory has two distinct strong-coupling points. One,



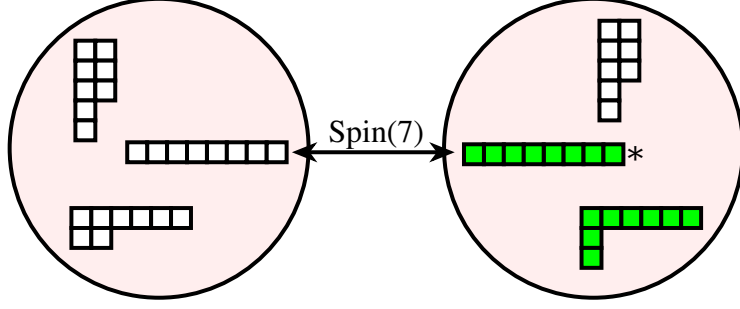
is a G_2 gauge theory, with matter in the $2(7) + 1$, coupled to the $(E_7)_8$ SCFT. Aside from the addition of the free hypermultiplet, this was example 10 of Argyres and Wittig [2].

The other strong coupling point of this theory,

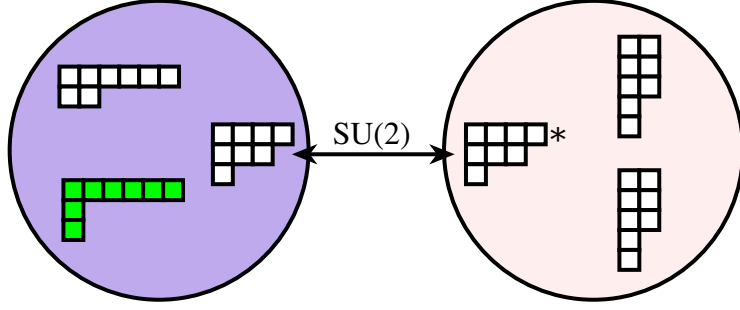


is an $SU(2)$ gauge theory coupled to the $Sp(4)_8 \times Sp(2)_7$ SCFT. The fixture on the right is empty; the mixed-fixture on the left provides both the SCFT and an additional free hypermultiplet.

As a second example, consider



This is a $Spin(7)$ gauge theory, with matter in the $4(8) + (7) + (1)$. The S-dual theory



is an $SU(2)$ gauge theory. The fixture on the right contributes a half-hypermultiplet in the fundamental. The fixture on the left is the $Sp(4)_8 \times Sp(2)_7$ SCFT plus a single *free* hypermultiplet. We weakly gauge an $SU(2)$ subgroup of $Sp(2)_7 \subset G_X$. From both points of view, we reproduce

$$G_{\text{global}} = Sp(4)_8 \times SU(2)_7 + 1 \text{ free hypermultiplet}$$

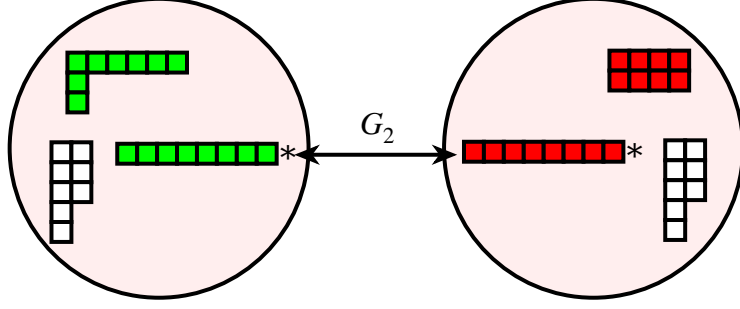
A third example is provided by the S-dual of $Spin(8)$ gauge theory with matter in the $4(8_s) + 2(8_c)$. This is discussed in section §4.4.

3.3.2. $Sp(5)_7$ SCFT

The other “new” SCFT is the $Sp(5)_7$ SCFT. It has $(a, c) = (\frac{41}{12}, \frac{49}{12})$ and a Coulomb branch of graded dimension $(d_2, \dots, d_6) = (0, 0, 0, 0, 1)$. The global symmetry group is $Sp(5)_7$.

The $Sp(5)_7$ SCFT appears twice on our list, once accompanied by 3 hypermultiplets (transforming as the $\frac{1}{2}(1; 1; 2, 1, 1) + \frac{1}{2}(1; 1; 1, 2, 1) + \frac{1}{2}(1; 1; 1, 1, 2)$ of the manifest $SU(2) \times SU(2) \times SU(2)^3$ associated to the punctures), and once (3 fixtures) accompanied by 4 hypermultiplets (transforming as the $\frac{1}{2}(1; 4; 1) + \frac{1}{2}(4; 1; 1)$ of the manifest $Sp(2) \times Sp(2) \times SU(2)$ associated to the punctures).

Let’s look at some examples of the $Sp(5)_7$ SCFT. Consider the 4-punctured sphere

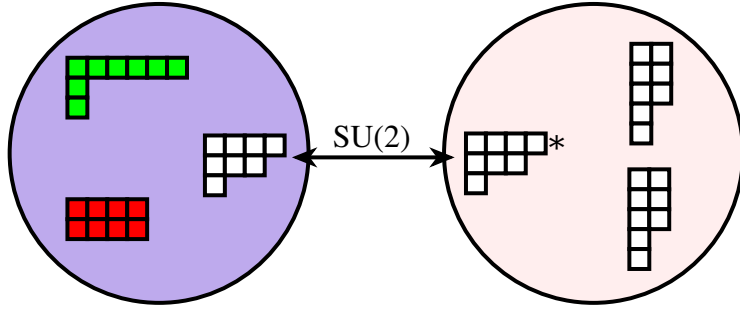


Both fixtures provide 2 hypers in the 7 of G_2 , plus 2 free hypers, so the 4-punctured sphere represents the G_2 theory with 4 hypers in the 7, plus 4 free hypers.

$$G_{\text{global}} = Sp(4)_7 + 4 \text{ free hypers}$$

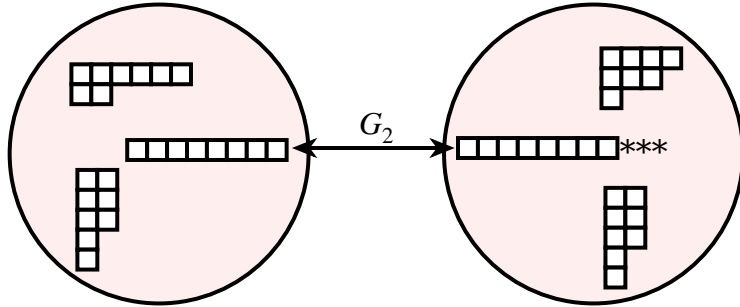
Aside from the 4 free hypers, this is example 4 of Argyres-Wittig [2].

The S-dual theory is



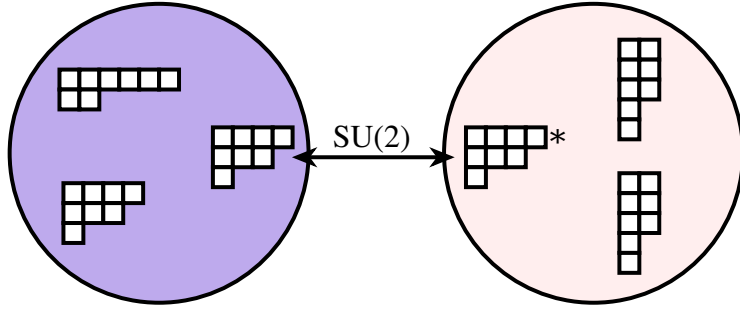
The fixture on the left is the $Sp(5)_7$ SCFT, with 4 free hypers. The fixture on the right contributes a half-hyper in the fundamental of $SU(2)$. Gauging an $SU(2) \subset Sp(5)_7$, yields the expected $Sp(4)_7$ global symmetry group of the S-dual of G_2 with 4 fundamentals.

As another example, consider the 4-punctured sphere



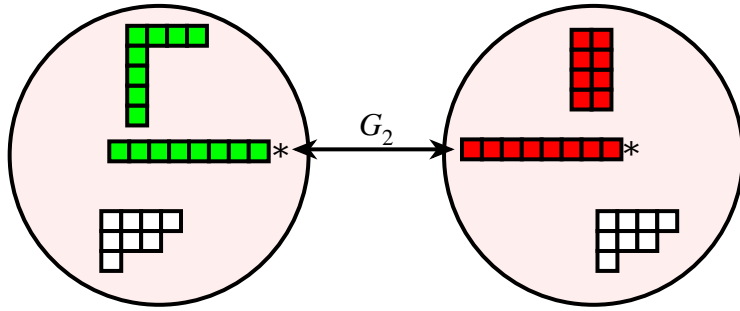
Here the fixture on the left represents 3 hypers in the 7 of G_2 plus 3 free hypers, and the fixture on the right represents 1 hyper in the 7. Notice that the G_2 cylinder in this example is different from the one in the previous example.

S-dualizing, we obtain



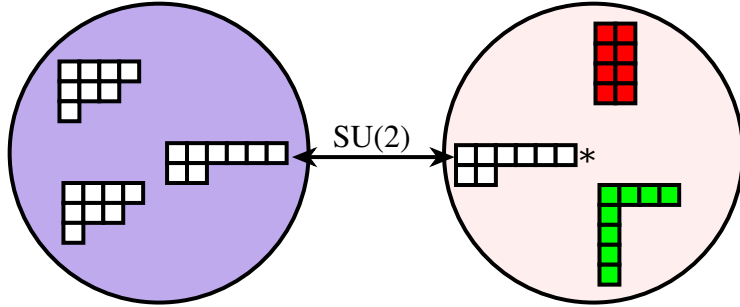
The fixture on the left is the $Sp(5)_7$ SCFT, where we gauge an $SU(2) \subset Sp(5)$, accompanied by 3 free hypers. The fixture on the right contributes 1 fundamental half-hyper.

A third example, also involving G_2 , is



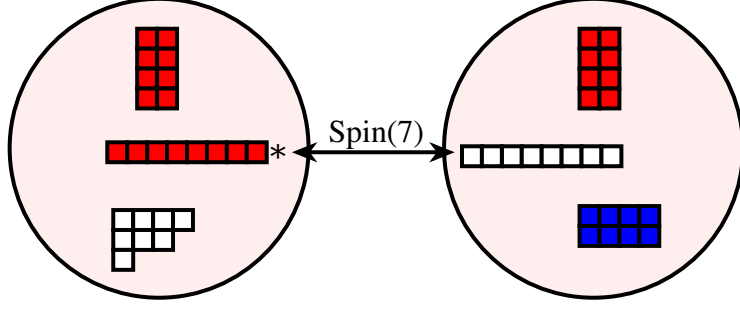
This is G_2 with 4 fundamentals and *two* free hypermultiplets.

The S-dual is



The fixture on the right is empty. The fixture on the left is, again the $Sp(5)_7$ SCFT, with one hypermultiplet transforming as a half-hyper in the fundamental of $SU(2)$ and two free hypermultiplets.

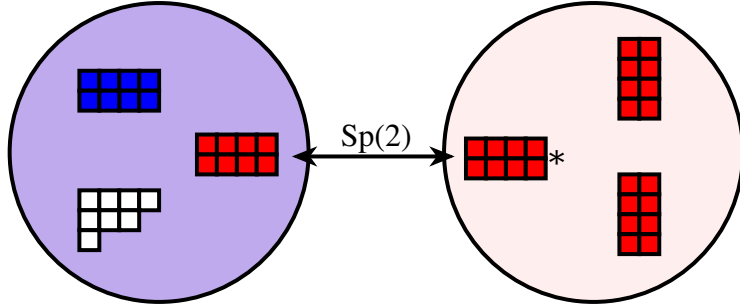
For a non- G_2 -related example, consider



The fixture on the left contributes hypermultiplets in the $2(7) + 1$. The fixture on the right is an $8_s + 2(8_c)$, considered as a representation of $Spin(8)$. Under the chosen embedding of $Spin(7)$, the 8_s decomposes as $7 + 1$, which the 8_c (and also the 8_v) decomposes as the 8 . So, all-in-all, this is a $Spin(7)$ gauge theory, with matter in the $3(7) + 2(8) + 2(1)$, so

$$G_{\text{global}} = Sp(3)_7 \times Sp(2)_8 + 2 \text{ free hypers}$$

The S-dual theory is



The fixture on the right contribute 2 hypermultiplets in the fundamental of $Sp(2)$. The fixture on the left is the $Sp(5)_7$ SCFT, accompanied by 4 hypermultiplets, two of which form an additional half-hypermultiplet in the fundamental of $Sp(2)$ and two of which are free. Altogether, there are 5 half-hypermultiplets in the fundamental, yielding the $Spin(5) = Sp(2)_8$ factor in G_{global} . Gauging the $Sp(2) \subset Sp(5)_7$ yields the remaining $Sp(3)_7$. This is example 5 of Argyres and Wittig [2].

4. $Spin(8)$ Gauge Theory

$Spin(8)$ gauge theory — with n_s hypermultiplets in the 8_s , n_c hypermultiplets in the 8_c and n_v hypermultiplets in the 8_v — has vanishing β -function for $n_s + n_c + n_v = 6$. The global symmetry group is

$$G_{\text{global}} = Sp(n_s)_8 \times Sp(n_c)_8 \times Sp(n_v)_8$$

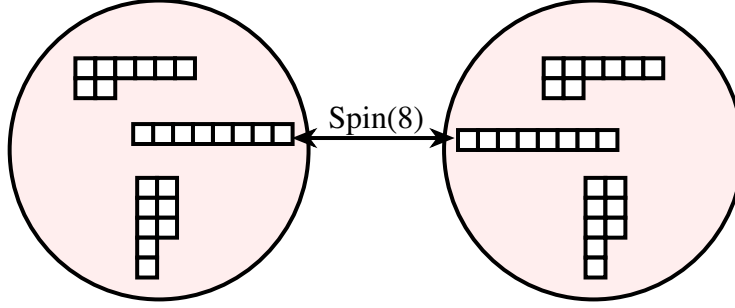
In the D_4 theory, all of the cases, with $n_{s,c,v} \leq 4$, are realized on the 4-punctured sphere. Up to $Spin(8)$ triality, this yields five different cases. We will discuss each of them, in turn, and give the strong-coupling behaviour in each case.

For the cases of $(n_s, n_c, n_v) = (3, 2, 1)$ and $(3, 3, 0)$, Argyres and Wittig [2] conjectured a strong-coupling dual. We find that each of these cases has *two* distinct strong-coupling limits. In each case, the conjecture of Argyres and Wittig corresponds to one of the two strong-coupling limits, that we find.

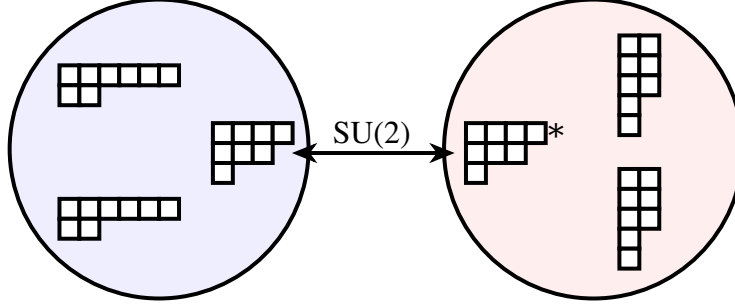
4.1. $2(8_s) + 2(8_c) + 2(8_v)$

The dual of $Spin(8)$, with matter in the $2(8_s) + 2(8_c) + 2(8_v)$, is an $SU(2)$ gauge theory, coupled to a half-hypermultiplet in the fundamental, and to the $Sp(2)_8^3 \times SU(2)_7$ SCFT.

One realization is

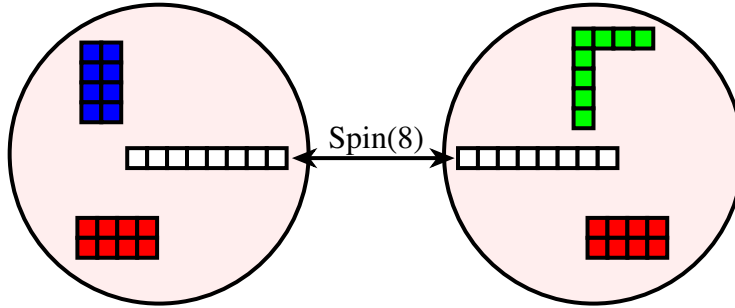


Each fixture contributes one $(8_v + 8_s + 8_c)$. The S-dual theory is

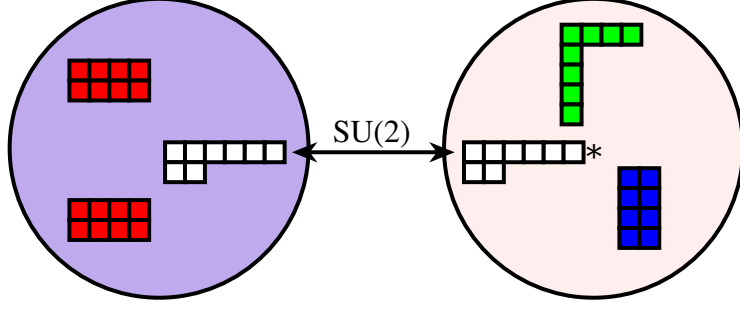


where the fixture on the right is a half-hypermultiplet in the fundamental of $SU(2)$, and the fixture on the left is the $Sp(2)_8^3 \times SU(2)_7$ SCFT.

Another realization of the same theory is



Here, the fixture on the left contributes $8_s + 2(8_c)$, and the fixture on the right contributes $8_s + 2(8_v)$. The S-dual is

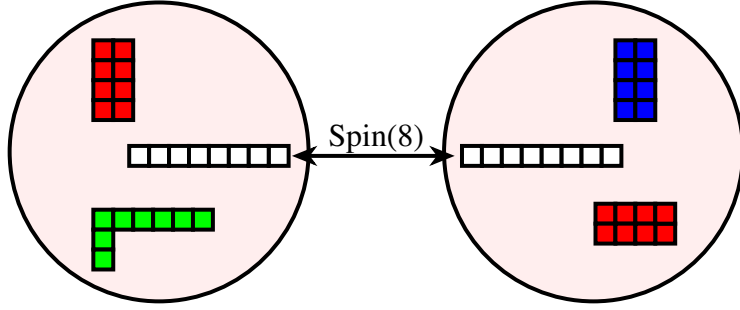


The fixture on the right is empty; the fixture on the left is the $Sp(2)_8^3 \times SU(2)_7$ SCFT plus a half-hypermultiplet in the fundamental of $SU(2)$.

4.2. $3(8_s) + 2(8_c) + 8_v$

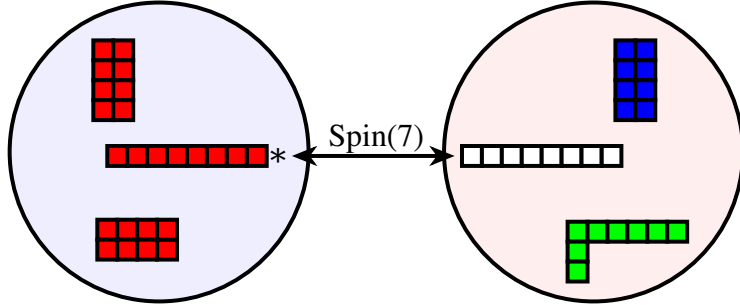
$Spin(8)$ gauge theory, with matter in the $3(8_s) + 2(8_c) + 8_v$, has two *distinct* strong-coupling limits. One is a $Spin(7)$ gauge theory, with matter in the $3(8)$, coupled to the $(E_7)_8$ SCFT. The other strong coupling limit is an $SU(2)$ gauging of the $Sp(3)_8^2 \times SU(2)_8$.

One realization is



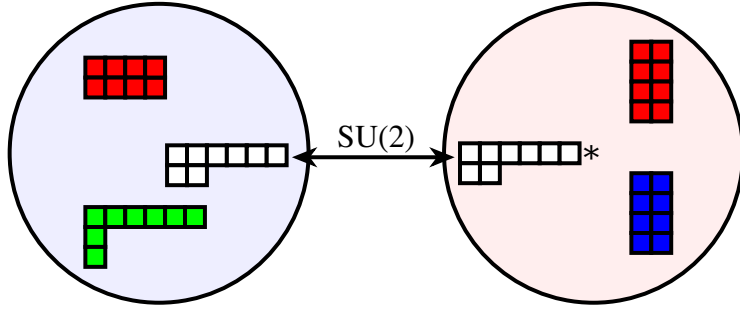
The fixture on the left contributes $2(8_s) + 8_v$, and the fixture on the right contributes $8_s + 2(8_c)$.

One of the corresponding strong-coupling points is given by



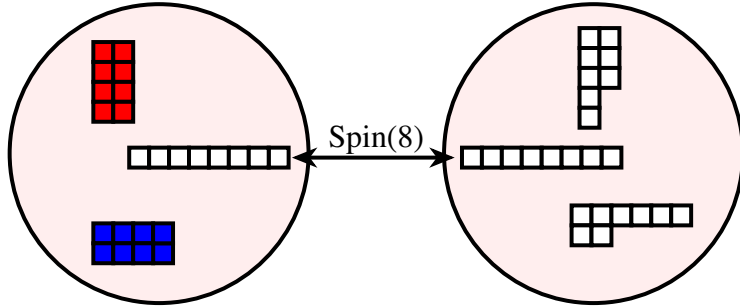
The fixture on the right yields matter in 3 copies of the 8; the fixture on the left is the $(E_7)_8$ SCFT.

The other strong coupling point is

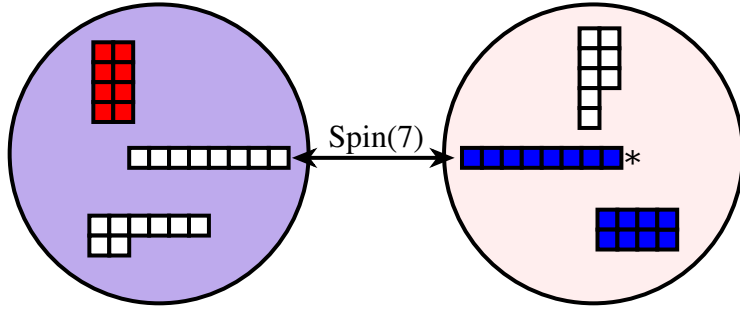


The fixture on the right is empty, while the fixture on the left is the $Sp(3)_8^2 \times SU(2)_8$ SCFT, where we gauge an $SU(2) \subset Sp(3)_8$.

Another realization of the same theory is

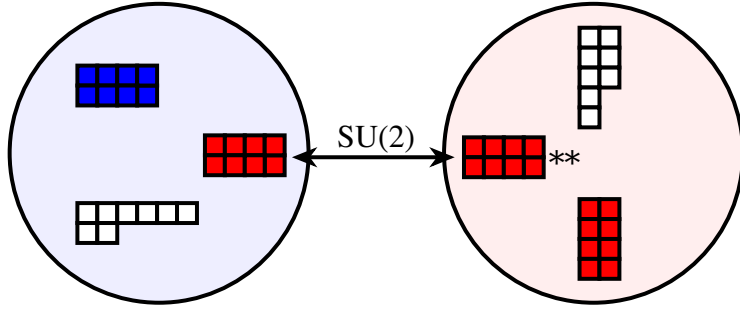


One strong coupling point is given by



The fixture on the right contribute 2 hypermultiplets in the 8 of $Spin(7)$. The fixture on the left is the $(E_7)_8$ SCFT plus an additional hypermultiplet in the 8.

The other strong coupling point is

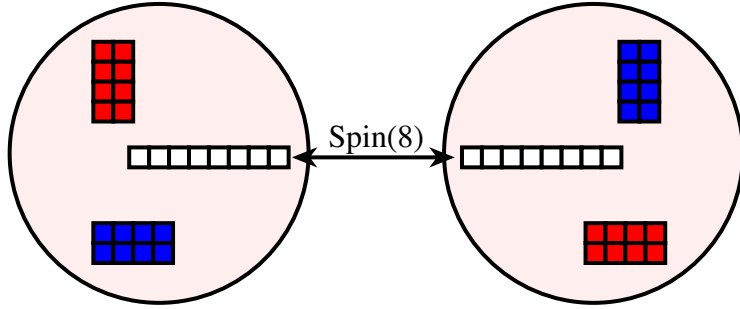


The fixture on the right is empty; the fixture on the left is, again, the $Sp(3)_8^2 \times SU(2)_8$ SCFT.

4.3. $3(8_s) + 3(8_c)$

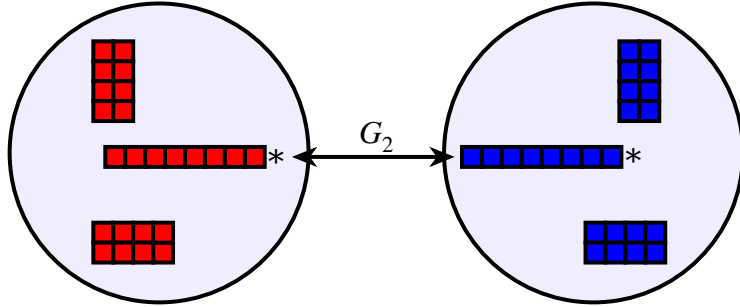
$Spin(8)$ gauge theory, with matter in the $3(8_s) + 3(8_c)$ also has two distinct strong coupling points. One is G_2 gauge theory, coupled to two copies of the $(E_7)_8$ SCFT. The other is an $SU(2)$ gauging of the $Sp(3)_8^2 \times SU(2)_8$ SCFT.

This is realized via



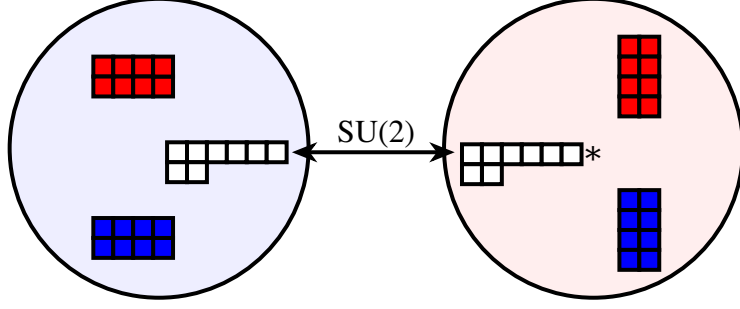
The fixture on the left yields $2(8_s) + 8_c$, while the figure on the right yields $8_s + 2(8_c)$.

One strong-coupling point is given by



Here, each fixture is a copy of the $(E_7)_8$ SCFT.

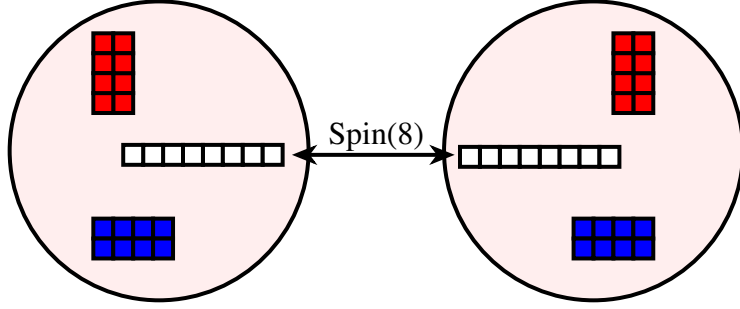
The other strong coupling point is



The fixture on the right is empty. The fixture on the left is the $Sp(3)_8^2 \times SU(2)_8$ SCFT where, this time, we gauge the $SU(2)_8$.

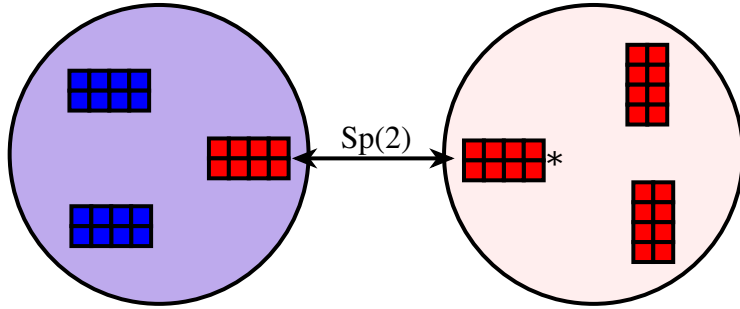
4.4. $4(8_s) + 2(8_c)$

$Spin(8)$, with matter in the $4(8_s) + 2(8_c)$ has, as its S-dual, an $Sp(2)$ gauge theory, with 5 half-hypermultiplets in the fundamental, coupled to the $Sp(4)_8 \times Sp(2)_7$ SCFT.



yields a $Spin(8)$ gauge theory, with matter in the $4(8_s) + 2(8_c)$.

The S-dual theory is

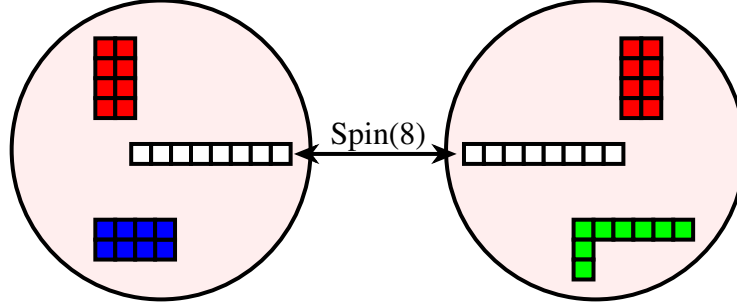


The fixture on the right contributes two hypermultiplets in the fundamental. The fixture on the left is the $Sp(4)_8 \times Sp(2)_7$ with an additional half-hypermultiplet in the fundamental of $Sp(2)$. Since there are, in total, five half-hypermultiplets in the fundamental, the flavour symmetry associated to the matter is $Spin(5) = Sp(2)_8$; the rest of G_{global} comes from the $Sp(4)_8 \subset Sp(4)_8 \times Sp(2)_7$.

4.5. $4(8_s) + 8_c + 8_v$

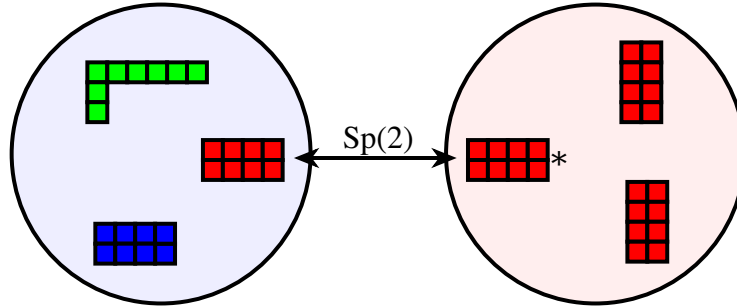
Finally, $Spin(8)$ gauge theory, with matter in the $4(8_s) + 8_c + 8_v$ has, as its S-dual, an $Sp(2)$ gauge theory, with 2 hypermultiplets in the fundamental, coupled to the $Sp(6)_8$ SCFT.

The $Spin(8)$ gauge theory can be realized as



where the fixture on the left gives matter in the $2(8_s) + 8_c$ and the fixture on the right gives matter in the $2(8_s) + 8_v$.

The S-dual is



The fixture on the right is 2 fundamental hypermultiplets of $Sp(2)$, which contribute the $Spin(4) = SU(2)_8^2$ factor to the global symmetry group. The fixture on the left is the $Sp(6)_8$ SCFT.

4.6. Seiberg-Witten curves

It is straightforward to compute the Seiberg-Witten curves, associated to any of these theories, in the form (3)

$$0 = \lambda^{2N} + \sum_{k=1}^{N-1} \lambda^{2(N-k)} \phi_{2k}(y) + \tilde{\phi}^2(y)$$

For instance, for $Spin(8)$ gauge theory, with hypermultiplets in the $3(8_v) + 3(8_s)$, imposing

the constraints, at each of the punctures, yields

$$\begin{aligned}
\phi_2(y) &= \frac{u_2 (dy)^2}{(y - y_1)(y - y_2)(y - y_3)(y - y_4)} \\
\phi_4(y) &= \frac{[u_4 (y - y_2)(y - y_3) - 2\tilde{u} (y - y_1)(y - y_4) + u_2^2 (y - y_1)(y - y_3)/4](dy)^4}{(y - y_1)^3(y - y_2)^2(y - y_3)^3(y - y_4)^2} \\
\phi_6(y) &= \frac{[u_6 (y - y_2) + u_2 \tilde{u} (y_1 - y_2)](dy)^6}{(y - y_1)^4(y - y_2)^3(y - y_3)^4(y - y_4)^2} \\
\tilde{\phi}(y) &= \frac{\tilde{u} (dy)^6}{(y - y_1)^2(y - y_2)^2(y - y_3)^3(y - y_4)}
\end{aligned} \tag{39}$$

Here u_2, u_4, u_6 and \tilde{u} are the Coulomb branch parameters. The obvious $SL(2, \mathbb{C})$ symmetry means that the physics depends only on the cross-ratio

$$e(\tau) = \frac{(y_1 - y_2)(y_3 - y_4)}{(y_1 - y_3)(y_2 - y_4)}$$

The $e(\tau) \rightarrow 0$ limit is the weakly-coupled $Spin(8)$ gauge theory; $e(\tau) \rightarrow \infty$ is the weakly-coupled $SU(2)$ gauge theory and $e(\tau) \rightarrow 1$ yields the weakly-coupled G_2 gauge theory.

The other cases are equally-easy to write down. It would be interesting to compare these results with the Seiberg-Witten curves obtained in [23,24].

5. $Spin(7)$ Gauge Theory

$Spin(7)$, with n hypermultiplets in the 8 and $(5 - n)$ in the 7, also has vanishing β -function. Perhaps with the addition of some free hypermultiplets, we can realize the cases $n = 2, 3, 4, 5$ in the D_4 theory.

5.1. $2(8) + 3(7)$

This theory (with the addition of two free hypermultiplets) was one of the examples discussed in §3.3.2. The theory has two strong-coupling points.

- One is a G_2 gauge theory, with two hypermultiplets in the 7, coupled to the $(E_7)_8$ SCFT.
- The other is an $SU(2)$ gauge theory coupled to the $Sp(4)_8 \times Sp(2)_7$ SCFT.

5.2. $3(8) + 2(7)$

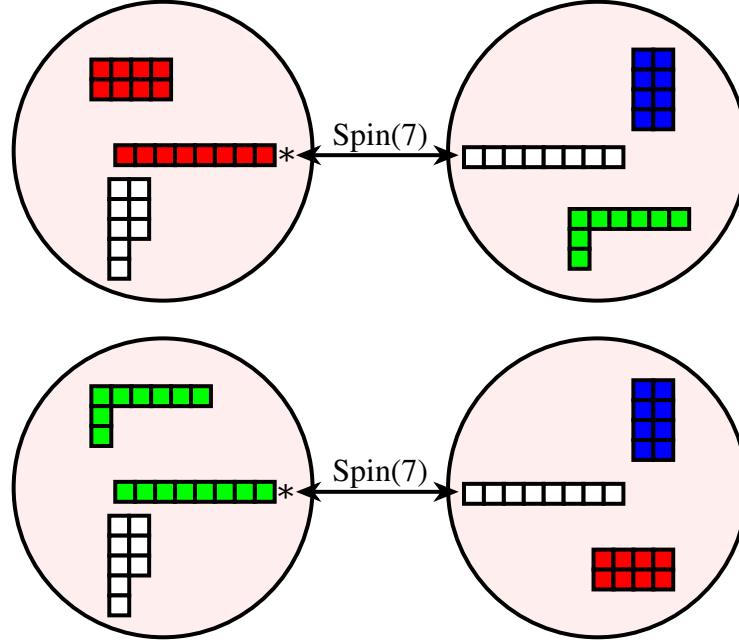
This theory (with the addition of two free hypermultiplets) was discussed in §3.3.1. The S-dual theory is an $Sp(2)$ gauge theory with 5 half-hypermultiplets in the 4, coupled to the $Sp(5)_7$ SCFT.

5.3. $4(8) + 1(7)$

This theory (with the addition of one free hypermultiplet) was also discussed in §3.3.1. The S-dual theory is an $SU(2)$ gauge theory with a half-hypermultiplet in the 2, coupled to the $Sp(4)_8 \times Sp(2)_7$ SCFT.

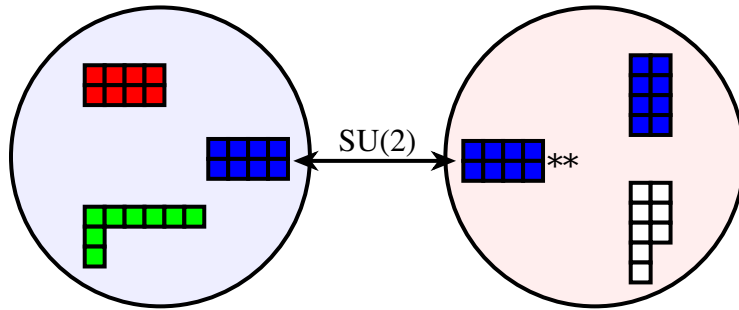
5.4. $5(8)$

This theory has three degeneration limits, two of which



are $Spin(7)$ gauge theories with matter in the $5(8)$. The fixture on the left contributes $2(8)$; the fixture on the right contributes $3(8)$.

The other degeneration,

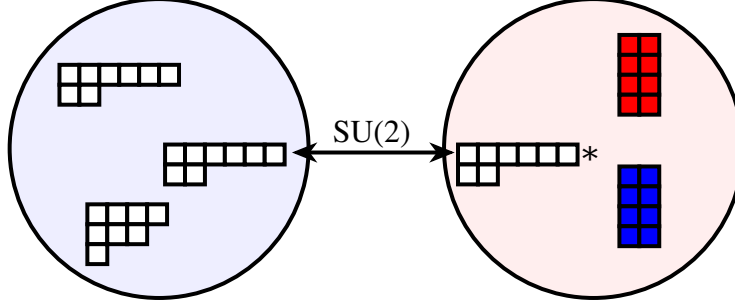


is an $SU(2)$ gauge theory coupled to the $Sp(6)_8$ SCFT (the fixture on the right is empty).

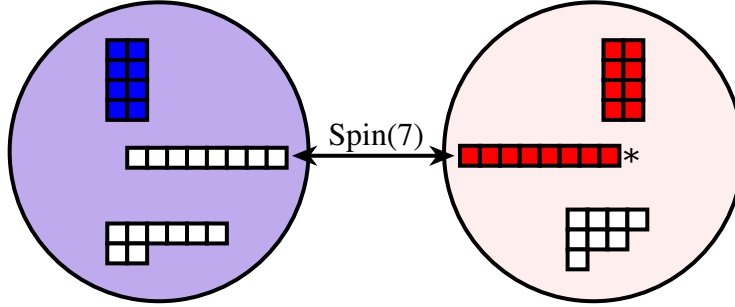
6. Other Interesting Examples

6.1. Fun with interacting SCFTs

Let's take the $Sp(2)_8^3 \times SU(2)_7$ SCFT and gauge an $SU(2)_8$ subgroup (the fixture on the right is empty):

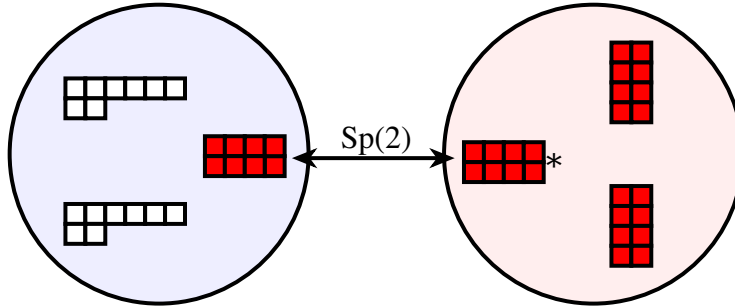


The S-dual theory is

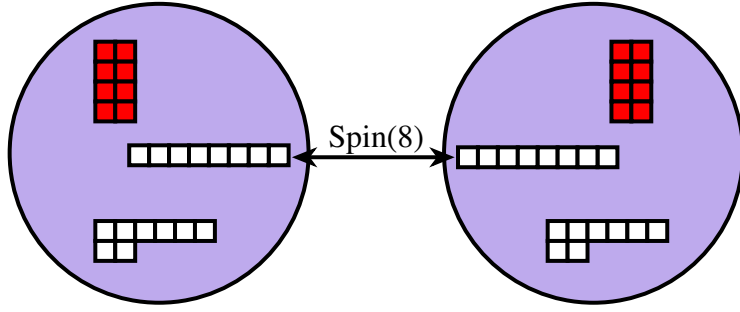


The fixture on the right contributes hypermultiplets in the $7 + 8$. The fixture on the left is the $(E_7)_8$ SCFT with matter in the 8_c of $Spin(8)$. Under the given embedding of $Spin(7)$, this matter transforms as an additional 8. So the matter contributes an $Sp(2)_8 \times SU(2)_7$ to the global symmetry group of the theory. The rest, $Sp(2)_8 \times SU(2)_8$, is the centralizer of $Spin(7) \subset E_7$.

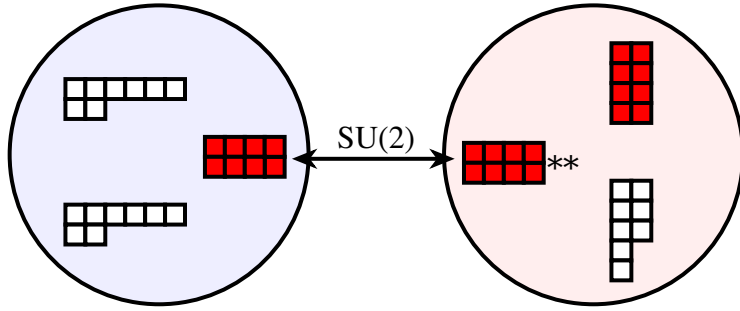
As another example of our methods, let us consider various gaugings of the $Sp(2)_8^2 \times SU(2)_4$ SCFT. We can gauge an $Sp(2)$ subgroup,



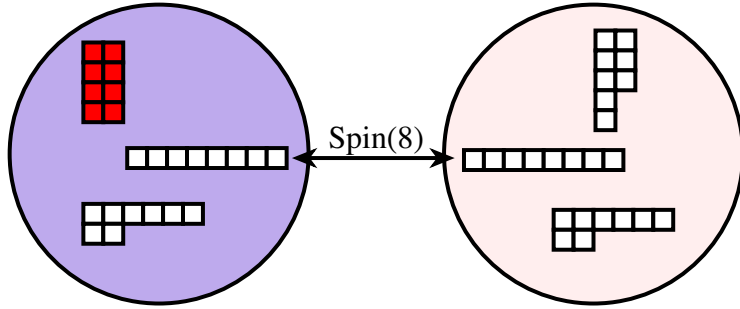
where the fixture on the right provides two hypermultiplets in the fundamental of $Sp(2)$. The S-dual theory,



is a $Spin(8)$ gauge theory, with matter in the $2(8_s)$, coupled to two copies of the $(E_7)_8$ SCFT.
 Instead, we can gauge an $SU(2)$ subgroup

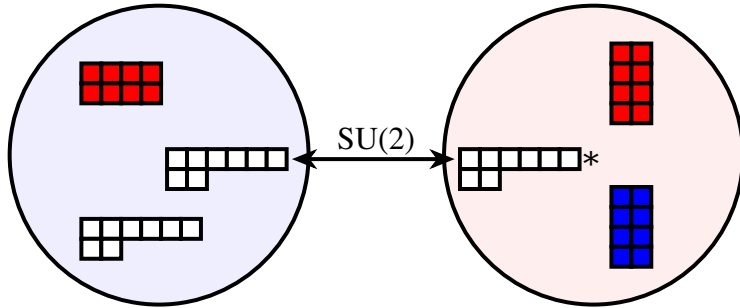


where the fixture on the right is empty. The S-dual

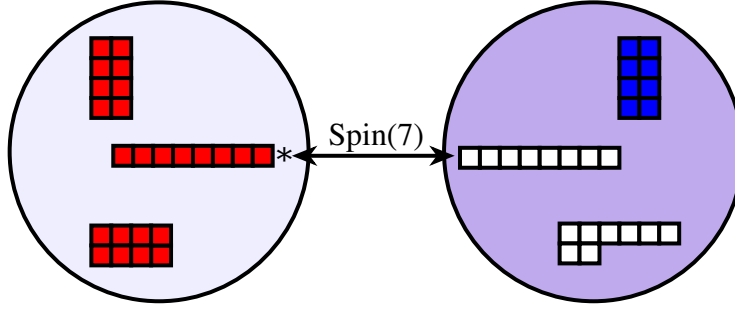


is a $Spin(8)$ gauge theory, with matter in the $2(8_s) + 8_c + 8_v$, coupled to one copy of the $(E_7)_8$ SCFT.

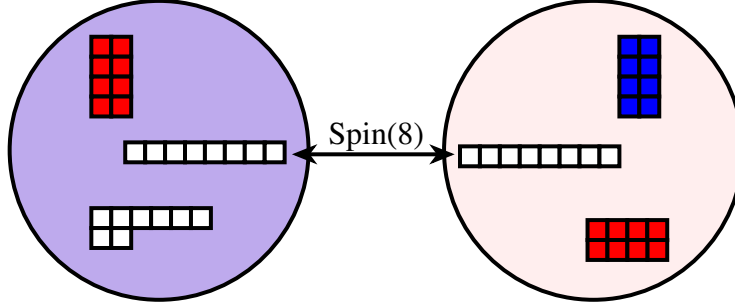
A different $SU(2)$ gauging of the $Sp(2)_8^2 \times SU(2)_8^4$ SCFT



has two distinct strong-coupling points. One,



is a $Spin(7)$ gauge theory, with matter in the 8, coupled to two copies of the $(E_7)_8$ SCFT. The other,

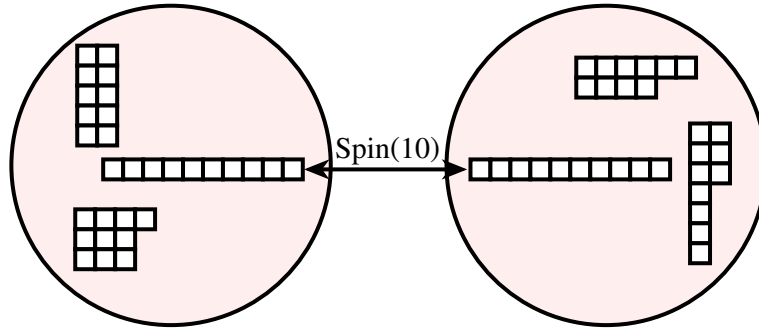


is a $Spin(8)$ gauge theory, with matter in the $2(8_s) + 2(8_c)$, coupled to a single copy of the $(E_7)_8$ SCFT.

6.2. D_5 example: $Spin(10)$ gauge theory

To further illustrate our methods, let us study *one* example from the D_5 theory, involving a $Spin(10)$ gauge theory with matter in the $3(16) + 2(10)$.

Start with the 4-punctured sphere

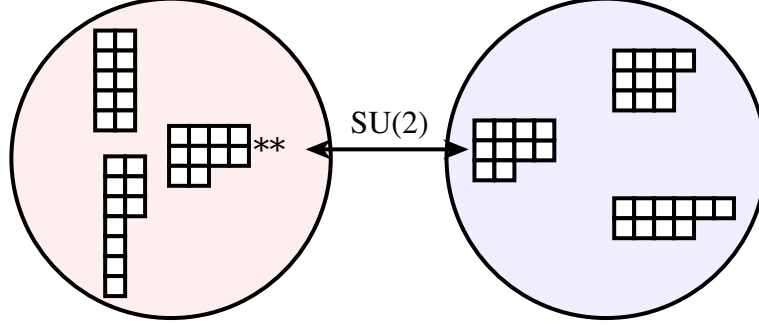



This is a $Spin(10)$ Lagrangian field theory with matter in the $3(16) + 2(10)$ representation. The left fixture provides 32 free hypermultiplets in the $(16, 2)$ of $Spin(10) \times SU(2)$, and the right fixture, 36 free hypermultiplets in the $(16, 1) + \frac{1}{2}(10, 4)$ of $Spin(10) \times Sp(2)$.

The global symmetry group of the theory is, thus,

$$G_{global} = SU(3)_{32} \times Sp(2)_{10} \times U(1),$$

This theory has two distinct strong coupling cusp points. One appears in the degeneration

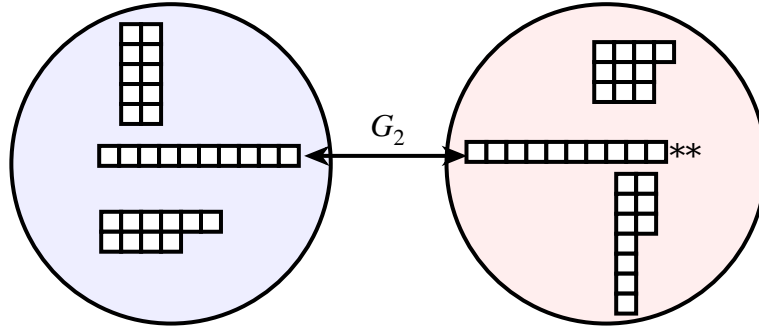


Here the left fixture is empty. The  irregular puncture has pole structure $\{1, 5, 7, 10; 6\}$, and imposes the constraint $c_{10}^{(8)} = (c_5^{(4)})^2$. The right fixture is an interacting SCFT with graded Coulomb branch dimension $d = (0, 0, 1, 1, 1, 0, 1)$ and global symmetry group

$$G_{SCFT} = Sp(2)_{10} \times SU(3)_{32} \times SU(2)_8 \times U(1),$$


and we gauge the $SU(2)_8$ subgroup.

The second strong coupling point appears in the remaining degeneration,



Here the fixture on the left is an SCFT with graded Coulomb branch dimension $d = (0, 0, 1, 1, 0, 0, 1)$ and global symmetry group

$$G_{SCFT} = (E_6)_{16} \times Sp(2)_{10} \times U(1),$$

and the fixture on the right is empty. The  irregular puncture has pole structure $\{1, 4, 5, 8; 5\}$. Under the decomposition $(E_6)_k \supset (G_2)_k \times SU(3)_{2k}$, we gauge a $(G_2)_{16} \subset (E_6)_{16}$.

Acknowledgements

The research of the authors is based upon work supported by the National Science Foundation under Grant No. PHY-0969020. The work of J. D. was also supported by the United States-Israel Binational Science Foundation under Grant #2006157. J. D. would like to thank the Erwin Schrödinger Institute, in Vienna, for hospitality while this manuscript was completed. We have benefited tremendously from conversations with Andrew Neitzke and Yuji Tachikawa, as well as well from some useful remarks of David Ben-Zvi.

A. Appendix: Nilpotent orbits in $\mathfrak{so}(2N)$

Here we lay out our conventions for nilpotent orbits in $\mathfrak{so}(2N)$. For more details, see [15]. We take $\mathfrak{so}(2N)$ to consist of block matrices of the form

$$\begin{pmatrix} A & B \\ C & -A^t \end{pmatrix} \quad (40)$$

where A, B, C are $n \times n$ matrices and $B^t = -B$, $C^t = -C$. Nilpotent orbits are in 1-1 correspondence with embeddings $\rho : \mathfrak{sl}(2) \hookrightarrow \mathfrak{so}(2N)$, up to conjugation. Here, $\mathfrak{sl}(2)$ is generated by $\{H, X, Y\}$ satisfying

$$[H, X] = 2X, \quad [H, Y] = -2Y, \quad [X, Y] = H \quad (41)$$

and we take $\rho(X)$ (which we will, henceforth, simply denote by X) as our representative element of the nilpotent orbit.

As noted in the text, a nilpotent orbit, in $\mathfrak{so}(2N)$, is specified by a D-partition of $2N$. Here, we will give our convention for assigning a triple of matrices of the form (40), satisfying (41), to such a partition.

Let e_1, e_2, \dots, e_n be the standard basis for \mathbb{C}^N . Let $E_{i,j}$ be the $2N \times 2N$ matrix with a 1 in the $(i, j)^{\text{th}}$ position and zeroes everywhere else. To the root, $e_i - e_j$, assign the matrix, of the form (40),

$$X_{i,j}^- = E_{i,j} - E_{j+N, i+N}$$

To the root $e_i + e_j$ (for $i < j$), assign

$$X_{i,j}^+ = E_{i, j+N} - E_{j, i+N}, \quad i < j$$

Also, let

$$H_i = E_{i,i} - E_{i+N, i+N}$$

- Take the D-partition, $[r_1, r_2, \dots]$, and divide it into pairs of the form $[r, r]$ and $[2s + 1, 2t + 1]$ ($s > t$). This is not quite unique: the D_6 partition, $[3, 3, 2, 2, 1, 1]$ can be divided into $[3, 3]$, $[2, 2]$, $[1, 1]$ or into $[2, 2]$, $[3, 1]$, $[3, 1]$. Different choices will result in different representatives of the same nilpotent orbit.
- To each pair of the form $[r, r]$, assign a block of r consecutive basis vectors of \mathbb{C}^N . We'll denote those by (e_1, e_2, \dots, e_r) , but they might be, say, $(e_{17}, e_{18}, \dots, e_{16+r})$. To each pair of the form $[2s + 1, 2t + 1]$, assign a block of $s + t$ consecutive basis vectors of \mathbb{C}^N . The blocks, thus assigned, must be non-overlapping, and will exhaust e_1, \dots, e_N .
- For each pair of the form $[r, r]$, let

$$\begin{aligned}
H &= \sum_{k=1}^r (r+1-2k)H_k \\
X &= \sum_{k=1}^{r-1} \sqrt{k(r-k)}X_{k,k+1}^- \\
Y &= X^t
\end{aligned}$$

- For pairs of the form $[2s+1, 2t+1]$, the general formula can be found in [15]. We'll just need the first few, for small values of t .

– For pairs of the form $[2s+1, 1]$, let

$$\begin{aligned}
H &= \sum_{k=1}^s 2(s+1-k)H_k \\
X &= \sum_{k=1}^{s-1} \sqrt{k(2s+1-k)}X_{k,k+1}^- + \sqrt{s(s+1)/2} (X_{s,s+1}^- + X_{s,s+1}^+) \\
Y &= X^t
\end{aligned}$$

– For pairs of the form $[2s+1, 3]$, let

$$\begin{aligned}
H &= \sum_{k=1}^s 2(s+1-k)H_k + 2H_{s+1} \\
X &= \sum_{k=1}^{s-2} \sqrt{k(2s+1-k)}X_{k,k+1}^- \\
&\quad + \sqrt{(s-1)(s+2)}X_{s-1,s}^- + \sqrt{s(s+1)/2} (X_{s,s+2}^- + X_{s,s+2}^+) + (X_{s+1,s+2}^- - X_{s+1,s+2}^+) \\
Y &= X^t
\end{aligned}$$

- Add up the contributions to H, X, Y from each pair. The resulting triple, $\{H, X, Y\}$, will be our embedding of $\mathfrak{sl}(2)$ and X will be our representative of the nilpotent orbit, corresponding to this partition.

The one exception to this rule has to do with “very even” partitions and our red/blue nilpotent orbits.

- For the red orbit, follow the prescription above.
- For the blue orbit, replace every instance of $X_{i,N}^\mp$ with $X_{i,N}^\pm$ and replace every instance of H_N with $-H_N$. This has the effect of exchanging the roles of the two irreducible spinor representations and flips the sign of the Pfaffian, $\tilde{\phi}(y) \rightarrow -\tilde{\phi}(y)$.

References

- [1] O. Chacaltana and J. Distler, “Tinkertoys for Gaiotto duality,” *JHEP* **11** (2010) 099, [arXiv:1008.5203 \[hep-th\]](#).
- [2] P. C. Argyres and J. R. Wittig, “Infinite coupling duals of $N = 2$ gauge theories and new rank 1 superconformal field theories,” *JHEP* **01** (2008) 074, [arXiv:0712.2028 \[hep-th\]](#).
- [3] D. Gaiotto, “ $N = 2$ dualities,” [arXiv:0904.2715 \[hep-th\]](#).
- [4] D. Gaiotto, G. W. Moore, and A. Neitzke, “Wall-crossing, Hitchin systems, and the WKB approximation,” [arXiv:0907.3987 \[hep-th\]](#).
- [5] D. Gaiotto and J. Maldacena, “The gravity duals of $N = 2$ superconformal field theories,” [arXiv:0904.4466 \[hep-th\]](#).
- [6] D. Nanopoulos and D. Xie, “ $N = 2$ generalized superconformal quiver gauge theory,” [arXiv:1006.3486 \[hep-th\]](#).
- [7] D. Nanopoulos and D. Xie, “Hitchin equation, singularity, and $N = 2$ superconformal field theories,” *JHEP* **03** (2010) 043, [arXiv:0911.1990 \[hep-th\]](#).
- [8] Y. Tachikawa, “Six-dimensional D_N theory and four-dimensional $SO-USp$ quivers,” *JHEP* **07** (2009) 067, [arXiv:0905.4074 \[hep-th\]](#).
- [9] Y. Tachikawa, “ $N = 2$ S-duality via outer-automorphism twists,” *J. Phys.* **A44** (2011) 182001, [arXiv:1009.0339 \[hep-th\]](#).
- [10] F. Benini, Y. Tachikawa, and D. Xie, “Mirrors of 3d Sicilian theories,” *JHEP* **09** (2010) 063, [arXiv:1007.0992 \[hep-th\]](#).
- [11] J. A. Minahan and D. Nemeschansky, “Superconformal fixed points with E_n global symmetry,” *Nucl. Phys.* **B489** (1997) 24–46, [arXiv:hep-th/9610076](#).
- [12] P. C. Argyres and N. Seiberg, “S-duality in $N = 2$ supersymmetric gauge theories,” *JHEP* **12** (2007) 088, [arXiv:0711.0054 \[hep-th\]](#).
- [13] K. Landsteiner, E. Lopez, and D. A. Lowe, “ $N = 2$ supersymmetric gauge theories, branes and orientifolds,” *Nucl. Phys.* **B507** (1997) 197–226, [arXiv:hep-th/9705199](#).
- [14] A. Brandhuber, J. Sonnenschein, S. Theisen, and S. Yankielowicz, “M-theory and Seiberg-Witten curves: Orthogonal and symplectic groups,” *Nucl. Phys.* **B504** (1997) 175–188, [arXiv:hep-th/9705232](#).
- [15] D. H. Collingwood and W. M. McGovern, *Nilpotent Orbits in Semisimple Lie Algebras*. Van Nostrand Reinhold, New York, 1993.
- [16] E. Witten, “An $SU(2)$ anomaly,” *Phys. Lett.* **B117** (1982) 324–328.

- [17] D. Nanopoulos and D. Xie, “More three dimensional mirror pairs,” *JHEP* **05** (2011) 071, [arXiv:1011.1911 \[hep-th\]](#).
- [18] S. Gukov and E. Witten, “Gauge theory, ramification, and the geometric Langlands program,” [arXiv:hep-th/0612073](#).
- [19] K. Hori, “Consistency condition for fivebrane in M-theory on $\mathbb{R}^5/\mathbb{Z}_2$ orbifold,” *Nucl. Phys.* **B539** (1999) 35–78, [arXiv:hep-th/9805141](#).
- [20] O. Chacaltana, J. Distler, and Y. Tachikawa. Work in progress.
- [21] H. Osborn and A. C. Petkos, “Implications of conformal invariance in field theories for general dimensions,” *Ann. Phys.* **231** (1994) 311–362, [arXiv:hep-th/9307010](#).
- [22] S. M. Kuzenko and S. Theisen, “Correlation functions of conserved currents in $N = 2$ superconformal theory,” *Class. Quant. Grav.* **17** (2000) 665–696, [arXiv:hep-th/9907107](#).
- [23] M. Aganagic and M. Gremm, “Exact solutions for some $N = 2$ supersymmetric $SO(N)$ gauge theories with vectors and spinors,” *Nucl. Phys.* **B524** (1998) 207–223, [arXiv:hep-th/9712011](#).
- [24] S. Terashima and S.-K. Yang, “Seiberg-Witten geometry with various matter contents,” *Nucl. Phys.* **B537** (1999) 344–360, [arXiv:hep-th/9808022](#).